

Analysis and mathematical modelling of industrial truck silencers

Marcus Johansson
Björn Nordle
mjo@msi.vxu.se, bjorn.nordle@gmail.com

Marcus Johansson
Björn Nordle
mjo@msi.vxu.se, bjorn.nordle@gmail.com

Analysis and mathematical modelling of industrial truck silencers

Master of Science Thesis

Mathematics and Acoustics

2007

Abstract

The currently low requirements on sound emissions for industrial trucks are expected to be raised in the near future. The company Kalmar Industries AB, which develop, produce and market industrial trucks, want to improve their truck silencers as a precaution to the future harder restrictions and also to improve their competitiveness. The sound emission produced by a vehicle depends on type and range of application it is designed for but the dominant part of the sound is usually produced by the engine and silencer.

A new measuring method is developed for studying sound emanating through the silencer system. The analysis of the measurement data establishes that the silencers are not working well. The simulations made with SIDLAB, which is a computer programme for calculating the propagation of sound in ducts, confirms that the silencers are inefficient and that they are simply too small.

A simulation which implements a parallel resonator in the main silencer shows that it is possible to make great improvements in reducing the noise from the truck as well as meeting requirements on space.

Mathematical modelling based on linearity and one-dimensional interaction between the silencer elements is advantageous and gives very good results when understanding, analysing and simulating the silencer. The simulation tool SIDLAB works well and saves a lot of time by its fast modelling and easy interface.

Key-words: Kalmar Industries, muffler, SIDLAB, forklift, industrial truck, silencer, sound analysis, modelling of sound in ducts.

Contents

1	Introduction	1
2	Measurements of silencers	2
2.1	Specifications	2
2.1.1	Measurements introduction	2
2.1.2	Environment and limitations	2
2.1.3	The silencers	4
2.1.4	Measurement equipment	4
2.1.5	Arrangement	4
2.1.6	Execution	5
2.2	Analysis	6
2.2.1	Sound power level and sound pressure level	6
2.2.2	Insertion loss	6
2.2.3	The difference between mic1, mic2 and mic3	7
2.2.4	The difference between the microphone positions 0.5 m and 1.5 m	9
3	Analysis of measurements on the silencers	10
3.1	Concerning the analysis and its methods	10
3.2	The configurations	10
3.2.1	System without silencer, Sil0	10
3.2.2	Silencer 1, Sil1	13
3.2.3	Silencer 2, Sil2	16
3.2.4	Silencer 1+2, Sil1+2	16
3.3	Concluding words of the analysis	16
3.3.1	Summary	16
3.3.2	Comments	17
3.3.3	Sources of error in measurement	17
4	Acoustic theory of modelling a silencer	18
4.1	The wave equation in one dimension	18
4.2	One dimension	18
4.3	Ports and nodes	20
4.3.1	2-port	20
4.3.2	1-port	20
4.3.3	Node	21
4.4	Complete network	22
4.4.1	The Projection matrix	22
4.4.2	The G -matrix	23
4.5	Examples	25
4.5.1	Making an S -matrix	25
4.5.2	Expansion chamber	29
5	Modelling of silencer	30
5.1	Modelling background	30
5.2	Example from the SIDLAB manual	30
5.3	Modelling Sil1 and Sil1+2	32
5.4	Comparison between modelling and measurement	34
5.4.1	Sil1	34

5.4.2	Sil1+2	36
5.5	Improved Sil1	38
5.5.1	Axial and radial increase of volume	38
5.5.2	Parallel resonator	38
5.6	Concluding words of the modelling of a silencer	40
5.6.1	Results	40
5.6.2	Sources of error in the modelling	41
6	Summary of results	43
6.1	Measurement method	43
6.2	Analysis of measuring results	43
6.3	Modelling	43
A	Appendix	44
A.1	Temperature	44
	References	45

1 Introduction

Reducing sound emission is of interest for many companies since disturbing noise has negative influence on the work environment. For many vehicles an internal combustion engine is usually the main source of noise, which is also the case for industrial trucks. The greatest part of this noise is led through some sort of silencer. The currently low sound restrictions on these trucks are expected to be raised in the near future, thus making the silencers interesting objects to study.

To this day, many companies in the silencer business still uses trial and error method when developing new silencers. This method, being slow and inaccurate, is quite expensive. The modern approach is to use calculations to create a model before testing and, in contrast, is fast, accurate and eliminates faulty models.

The purpose of this thesis is to examine the silencers efficiency and to give examples of how to improve them. To reach these goals the simulation tool SIDLAB is used to provide computer models of the silencers and compare the results to the measured data. Kalmar Industries provided the task of improving their truck silencer and the Marcus Wallenberg Laboratory at Kungliga Tekniska Högskolan provided the simulation tool SIDLAB. These tasks put together will show that SIDLAB is very useful for understanding and improving silencers.

Chapter two explains the measurement setup and an discusses the various microphone positions.

The third chapter features an extensive analysis of the recorded sound from the different configurations. Internal and external sound sources are identified and the silencers efficiency is determined.

Chapter four provides some of the theory behind the simulation tool SIDLAB and starts with describing the wave equation in one dimension and is followed by how SIDLAB elements are theoretically connected.

In chapter five SIDLAB simulations are compared with the measured results from the third chapter. Also, different ideas of improving the silencers are presented.

The chapter six is a summary of achieved results.

2 Measurements of silencers

This chapter is comprised of a short description of the truck and how the actual testing was made. After that a description of the different microphone positions is conducted, considering both distance and angle in measurement.

2.1 Specifications

2.1.1 Measurements introduction

A six liter, six cylinder Volvo Penta engine (TAD 750 VE) with its two Dinex mufflers were the objects to be put under scrutiny. The measurements were performed partly to determine how the existing measurement procedure works and evaluate new improved microphone positions, and partly to get adequate data in order to perform the analysis of the two silencers.

2.1.2 Environment and limitations

The measurements were performed at Kalmar Industries own test area on which the truck was placed on even asphalt in an effort to avoid sources of disturbance, *i.e.*, echoes and other trucks being tested simultaneously. Weather conditions were good with calm winds, sunny skies and a temperature of approximately $-5\text{ }^{\circ}\text{C}$. Possible sources of reflection beside the ground were trees at a distance of 20 m from the truck. Subsequently no consideration was made concerning echoes or other disturbance besides the truck itself.



Figure 2.1: The Kalmar DCE 160-12, diesel.

A motor vehicle most often has several different sound sources (parts where sound is produced). Further, the truck on which measurements were made had hydraulics that made quite some noise that will be a small point of interest further on in the thesis. Also there exist air conditioning, tire noise and drivetrain as sources of sound on this truck. The drivetrain is assumed to produce most sound because the operating speed is too low

for the tires to produce any significant noise. The drivetrain can be divided into parts that can be viewed as separate sound sources as follows:

- oil pump
- valves
- engine fan
- turbo with intercooler and waste gate
- gearbox
- vibrations in the chassis and the cabin (amplification from the drivetrain vibrations)
- air intake sound
- acoustic leakage from mufflers and exhaust system
- exhaust.

All these sources contribute to the total sound emitted by the drivetrain and should be taken into consideration when reducing the sound that the truck makes. However, the focal point has been put on the sound made by the engine and led through the exhaust system since this is the most important thing when constructing an exhaust system. The problem with choice of materials and thickness has not been addressed.

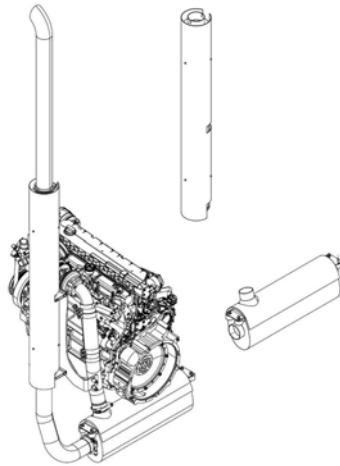


Figure 2.2: Left: Silencer system and engine. Top: Silencer 2. Right: Silencer 1.

2.1.3 The silencers

There are two mufflers available in the existing exhaust system. For further reference they have been given the names *Sil1* and *Sil2* and could be seen in figure 2.2. *Sil1* is the main silencer and consists mainly of a pair of volume resonators, perforations and mineral wool. *Sil2* is a complementary silencer that can be chosen by a customer requiring extra low sound emission. The *Sil2* design is intended for attenuating higher frequencies and is essentially just a lined duct, *i.e.*, a perforated pipe inside another larger pipe with mineral wool between the two. When measuring without these mufflers, replacing *Sil1* with a short piece of bent pipe and *Sil2* with a straight pipe, the system is referenced to as *Sil0*. The bent pipe is seen in figure 2.3. The length of the bent pipe is 0,25 m and length of the straight pipe is the same as silencer 2. The system containing both *Sil1* and *Sil2* is referenced as *Sil1+2*.



Figure 2.3: The pipe replacing the main silencer, *Sil1*.

2.1.4 Measurement equipment

The measuring equipment used was a *Brüel & Kjær 3560 C* with the software *Pulse v.10.1*. In this mode it is possible to measure six channels of sound and/or vibration and one optional channel for the rotational speed of the engine. The microphones were of make *Brüel & Kjær 4181* and the acoustic reference *Brüel & Kjær 4231*. The measure range was 0-6400 Hz.

2.1.5 Arrangement

Based on the existing measurement position used by Kalmar Industries in prior measurement, 0.5 m from orifice and 45° angle in the horizontal plane, new microphone positions

were chosen. The new positions contains this point and in addition two new positions at 0.5 m and 45° angle in the horizontal plane but with vertical angles $\pm 45^\circ$ respectively. Three new points at the same angles but 1.5 m distance from the orifice were also used. This is explained further in chapter 2.2.4.

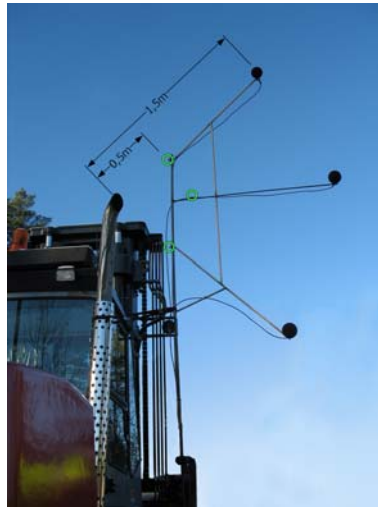


Figure 2.4: An illustration of the six positions.

The photograph in figure 2.4 is from the actual measurement and shows the microphones in the stand Kalmar Industries made for the occasion. Three microphones were used on every individual measurement. During each measurement the microphones were at the same radius and then moved on the stand to obtain a different distance. The microphone placements, top to bottom, are denoted *mic1*, *mic2* and *mic3*.

2.1.6 Execution

In order to get complete and credible data, measurements were made on all possible configurations. This means the three different rotational speeds of the engine, two microphone distances and three exhaust systems. This means $3 \times 2 \times 3 = 18$ configurations to be tested. Each measurement was carried out by using three microphones, *i.e.*, the sound pressure level was recorded from three positions with the same radius at the same time. (chapter 2.2.3, 2.2.4)

The choice of different rotational speeds of the engine was made to establish which mode was worth analysing. The three modes tested were low idle, high idle and lift. Low idle means that the engine was at idle; no revving. High idle means that the engine was revved up to about 2000 rpm without any load applied. Lift means that the engine was revved to its maximum working speed, slightly below high idle, 1980 rpm, and then a full working load of 12 tonnes was lifted by the forks to its maximum height. In advance the hypothesis was that the choice would fall upon lift and due to that lift has far superior sound levels, this mode is used throughout the rest of the thesis. The reasons for choosing lift are explained in chapter 3.1.

2.2 Analysis

This chapter contains analysis of the different microphone positions and if the microphones recording different sound pressure levels. The premier task is to investigate the three microphones at 1.5 m and how they differ in sound pressure level in any way. Secondly the effects of distance were looked upon all three microphones.

2.2.1 Sound power level and sound pressure level

Because the measurement was made in only three points at equal distance from the source (the exhaust orifice), there is no way of telling the exact sound power level. What can be done, however, is to measure sound pressure level from different muffler configurations in three points and calculate the difference. Coincidentally the difference in sound pressure level L_p is equal to the difference in sound power level L_w , both differences expressing the decrease in sound power level for sound parsing the silencer. The reason for the two levels being equivalent in such a fashion derives from the fact that the directivity by the orifice for the three systems are equivalent, *i.e.*, if the microphones are in the same points the sound will spread in the same fashion in any muffler configuration. Example: Muffler a produces $L_{pa} = 20 \log\left(\frac{p}{p_0}\right)$ with $p_0 = 2 \cdot 10^{-5}$ Pa [2], and is compared to a muffler b in the same system which gives L_{pb} . This gives $L_{pb} - L_{pa} = L_{wb} - L_{wa}$ regardless of L_{wa} and L_{wb} being known or not.

2.2.2 Insertion loss

There are two different ways to determine the efficiency of a muffler. They are transmission loss, D_{TL} and insertion loss, D_{IL} . D_{TL} is quite complicated, it involves measuring the sound power before and after a muffler/exhaust system. D_{IL} on the other hand compares two different systems *a* and *b* at an arbitrary point, suitably at a safe distance from gas flow and sources of disturbance. Hence it becomes very practical as limitations of choice are small. Thus, the insertion loss is a measurement of reduced or gained sound pressure level after changing the exhaust system and can be expressed as $D_{IL} = L_{pb} - L_{pa}$ which may be written as;

$$D_{IL} = 10 \log \left(\frac{p_b^2}{p_{ref}^2} \right) - 10 \log \left(\frac{p_a^2}{p_{ref}^2} \right) = 10 \log \left(\frac{p_b^2/p_{ref}^2}{p_a^2/p_{ref}^2} \right) = 20 \log \left(\frac{p_b}{p_a} \right). \quad (2.1)$$

Here, $D_{IL} = 20 \log(p_b/p_a)$ is the commonly accepted expression. Furthermore, the insertion loss D_{IL} is a practical measure for expressing the decrease in sound pressure level when installing the silencer and D_{IL} is because of that used in this thesis.

2.2.3 The difference between mic1, mic2 and mic3

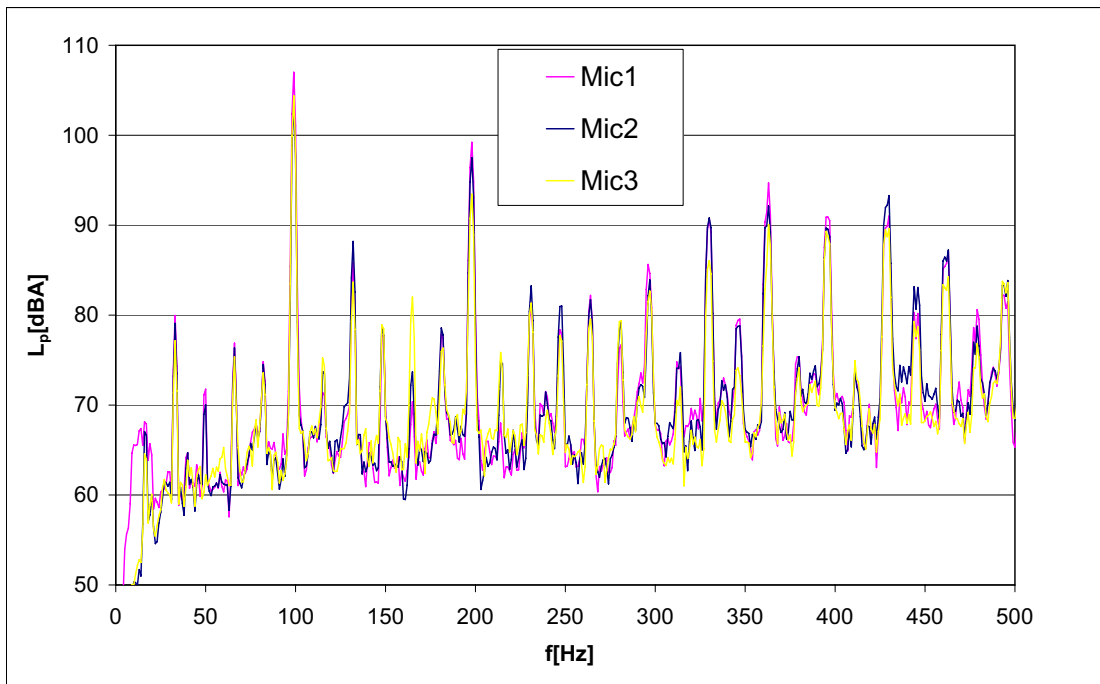


Figure 2.5: Measured sound pressure level with all three microphones at a distance of 1.5 m from the orifice. The engine is in lifting mode and Si10 is used. The frequency interval is 0-500 Hz.

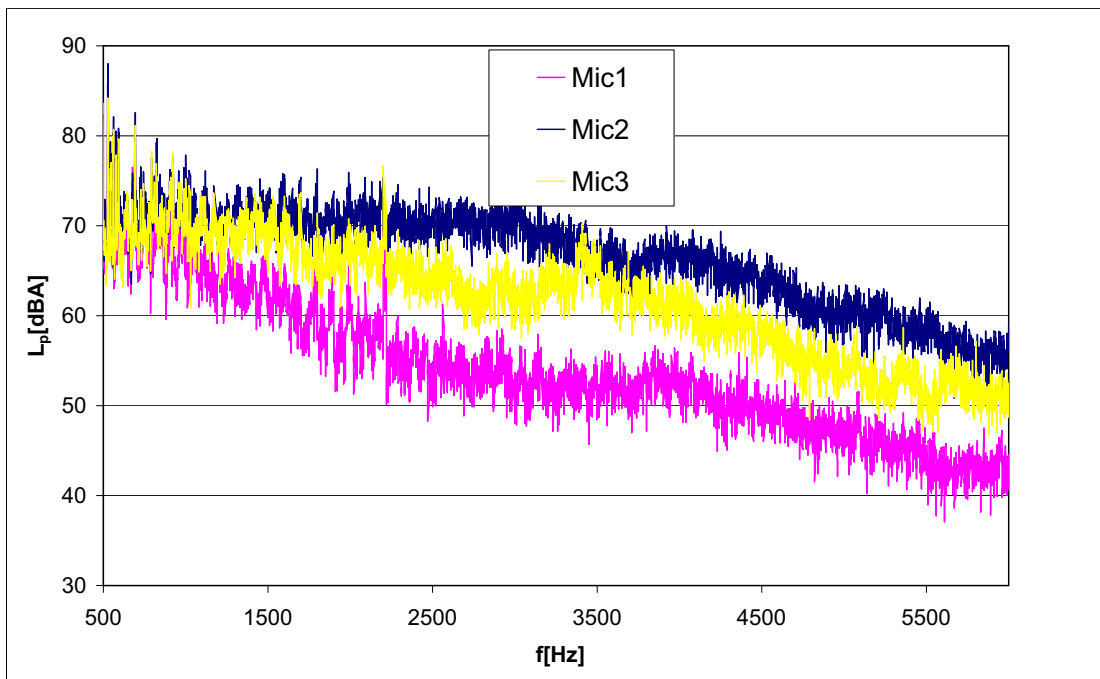


Figure 2.6: All three microphones at a distance of 1.5 m from the orifice. The engine is in lifting mode and Si10 is used. The frequency interval is 500-6000 Hz.

The graph in figure 2.5 shows the sound pressure level in the frequency interval 0-500 Hz at a distance of 1.5 m. In this graph no clear difference in level between the

microphones can be seen. It can be established that for low frequency sound all three microphones registers approximately the same sound pressure level. When the wave length is large compared to the pipe opening diameter the sound waves disperse spherically. In the graph in figure 2.5 the wave length is long and leads to a conformal spread in all directions for these frequencies. For the remaining interval, 500 Hz and up, graph 2.6 shows that mic2 has the highest sound pressure level, followed by mic3 and mic1 in falling order, where mic1 has the lowest sound pressure level. This is assumed to be related to the angle of the microphones to the exhaust flow direction. "If the frequency is high, thus making the wave length small compared to the opening, the sound wave will spread in a straight direction with shadows to the sides" [2]. In other words, the higher frequency a source emits the more directional the pattern will be. This means that for higher frequencies, *i.e.*, $f \gtrsim 4000$ Hz the microphone closest to the gas flow or acoustic flow will register higher pressure levels than the rest of the microphones for the high frequency sounds. Mic2 is therefore assumed to be closest to the directed high frequency noise than the other two microphones. However the differences are small and the assumption that all three microphones give equally important values and that it gives more to the future analysis a mean value from the three microphones will be used in the rest of the thesis. This should smooth out any irregularities or disturbances that might have influenced one of the microphones. The mean value is calculated as,

$$L_m = 10 \log \left[\frac{1}{3} (10^{0,1L_{p1}} + 10^{0,1L_{p2}} + 10^{0,1L_{p3}}) \right].$$

2.2.4 The difference between the microphone positions 0.5 m and 1.5 m

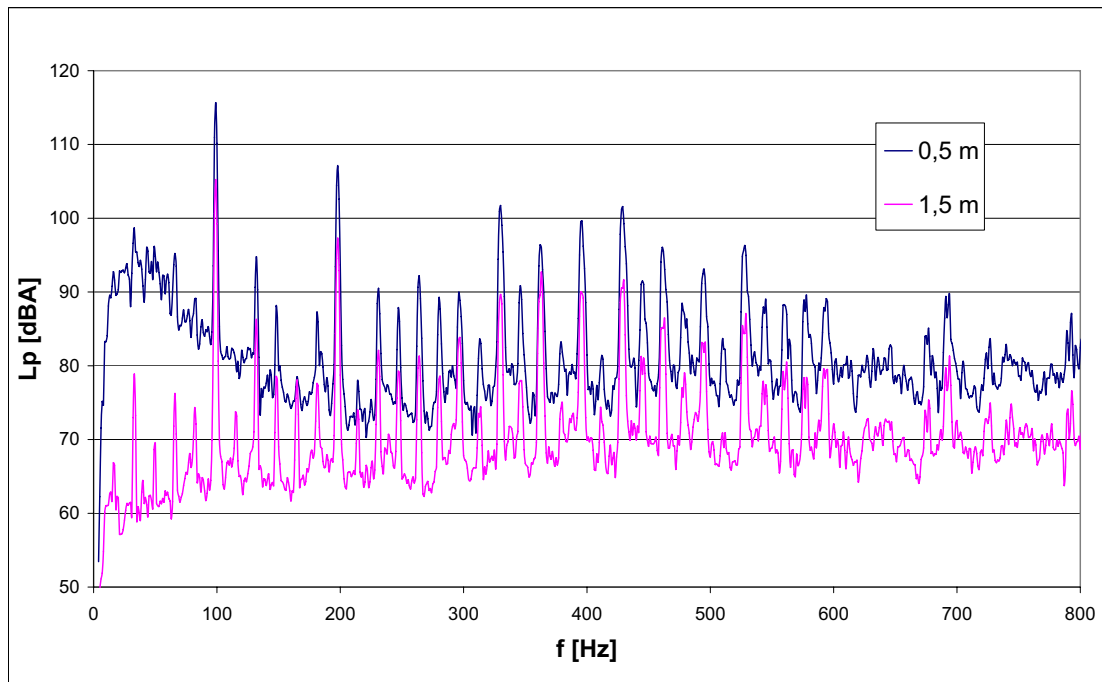


Figure 2.7: Measured sound pressure level at two different lengths from the orifice; 0.5m and 1.5m. The engine is in lifting mode and equipped with system containing Silo.

Two causes are interesting to analyse more closely since there are a few factors within the near field and external sound sources that can influence the final measuring results. Near field effects were found in figure 2.7. As expected the levels are higher in general for 0.5 m than 1.5 m due to the difference in distance. A close-up on the low frequencies tell a different tale since the levels at 0.5 m in figure 2.7 are very high, up to 35 dB higher than 1.5 m, between 0 Hz and 150 Hz. This corresponds to the term "acoustic near field" [2] which, in short, means that if $(2\pi r \ll \lambda)$ the sound pressure levels will be overestimated. This is the case at 0.5 m from the orifice and it is clearly not the ideal distance. This is why this thesis uses the distance of 1.5 m where frequencies should be much more than 36 Hz to minimize the near field effects. The 1.5 m function in figure 2.7 displays no signs of near field effects. Since the highest sound level is at 100 Hz the use of a 0.5 m distance, as Kalmar Industries currently does, can thus not be recommended. At a distance of 1.5 m the near field poses no source of error.

A drawback to using 1.5 m instead of 0.5 m is that the background noise is more dominating here and the further away from the truck one moves the background noise will be even more dominating.

It is assumed that externally created sound sources differ from the internal ones by not decreasing at the same rate when changing the radius. The first and easiest peak to observe is at 363 Hz, which proved to be one of two hydraulic pumps, used in the lift mode. This peak is replaced by a mean value of the adjacent frequencies. Further frequencies that can be assumed to originate from other sources are the 100 Hz and 200 Hz peaks, but since these are the engine's prime frequency respectively its double prime frequency it is assumed that these two peaks are strictly internal. To be able to make certain whether peaks are internal or external additional measurements must be made, taking the extra precaution of isolating the truck or choosing additional measure points.

3 Analysis of measurements on the silencers

This chapter explains how the actual measurement results are used and how they are interpreted. The graphs containing the measured sound are thoroughly examined to identify peaks. This is done by using different analysing techniques.

3.1 Concerning the analysis and its methods

To be able to conduct a frequency analysis and to study the measurements with respect to the frequency, a filter is needed when processing the signal data. Several filters exist for this purpose, which differ from each other. Depending on which frequency intervals that are supposed to be achieved, different filters are used. Kalmar Industries (KI) use the Fast Fourier Transform - method (FFT) when measuring sound pressure level. This gives KI discrete values that can easily be processed in a computer programme. When using FFT, a band pass filter is used. The band width does not vary along the frequency axis, which is why it is called an absolute bandwidth filter. Since the bandwidth of the FFT filter in this measurement is only 1 Hz regardless of frequency it can be helpful to use a constant relative filter instead. This can be done so that it produces an octave band filter or, as used in this thesis, a one third octave band filter. These bands are proportional to a middle frequency and the third octave filter has standardised bands [2]. However, these table values are not used in the thesis. Instead the middle frequencies are based on the definition $f_m = f_l \cdot (2)^{1/6} = f_u / (2)^{1/6}$, f_l =lower limit and f_u =upper limit. The middle frequencies are based and starting on the standard $f_m = 4$ which is calculated upwards producing middle frequencies near the standardised ones. Measurements were made on three different settings on the engine, but only one of these settings are taken in consideration when investigating the mufflers in this thesis. The setting that is taken in consideration is lift, which is based upon the following reasons:

- The sound pressure level is noticeably higher during lift than during low and high idle.
- The mean flow velocity in the pipes is much higher during lift than during low and high idle.
- KI specifies that the investigation should focus on speeds near 2000 rpm.
- The different insertion losses are highest in lift. This means that the existing mufflers are most efficient during lift.

Measurements were also made on two different distances from the orifice, 0.5 m and 1.5 m, but in this section the analysis of the silencer configurations is made on 1.5 m. The reason for this is described in chapter 2.2, where also more details about the near field are given. The sound pressure level and insertion loss are additionally transformed to third octave bands for all systems. This will give a clear understanding of the differences between the muffler systems.

3.2 The configurations

3.2.1 System without silencer, Sil0

Figure 3.1 demonstrates the character of the sound emitted from the orifice. The sound from Sil0 is not affected by any reactive or dissipative elements besides the length of pipes themselves with their different dimensions. Pipes are considered as reactive elements.

Points of interest here are frequencies that stands out from the crowd or, in other words, dominates the rest of the frequencies. Something should be mentioned here about sound pressure and sound pressure level. The scale for dB is logarithmic which means that high values of pressures receives a higher weight than a lower pressure value. A 6 dBA difference of sound pressure level constitutes twice the sound pressure in Pascal. When calculations of the sound pressure levels, of all the frequencies, are made it is therefore very important to include frequency peaks which are 15 dBA above the surrounding frequencies. Similarly, because low pressure values in Pascal receives low weight in dB, low frequencies are unimportant in the context. It is based partially on this that, in some graphs, frequencies below 51 Hz are excluded. Other than this the rest of the frequency interval is included from 0-6400 Hz.

f[Hz]	99	198	330	395	430	
(f_m)	(102)	(203)	(323)	(406)	(406)	Sum
L_p [dBA]	105	97	90	90	92	106

Table 3.1: Without silencer. Sound pressure level, L_p , and their middle frequency in parenthesis for the six most important frequencies and their logarithmic sum.

When observing only the peaks it is very clear that 99 Hz, with its 105 dBA, is very dominant. In figure 3.1 and table 3.3 it can be seen just how dominant. Adding the four next most dominating peaks, the logarithmic sum is just slightly higher. Above 1 KHz the sound pressure level stays below 85 dBA. At 363 Hz the measurement produces a peak while using Sil0, Sil1 as well as Sil1+2. This peak has been replaced with a mean value based on the surrounding sound pressure levels. This was done because it became clear

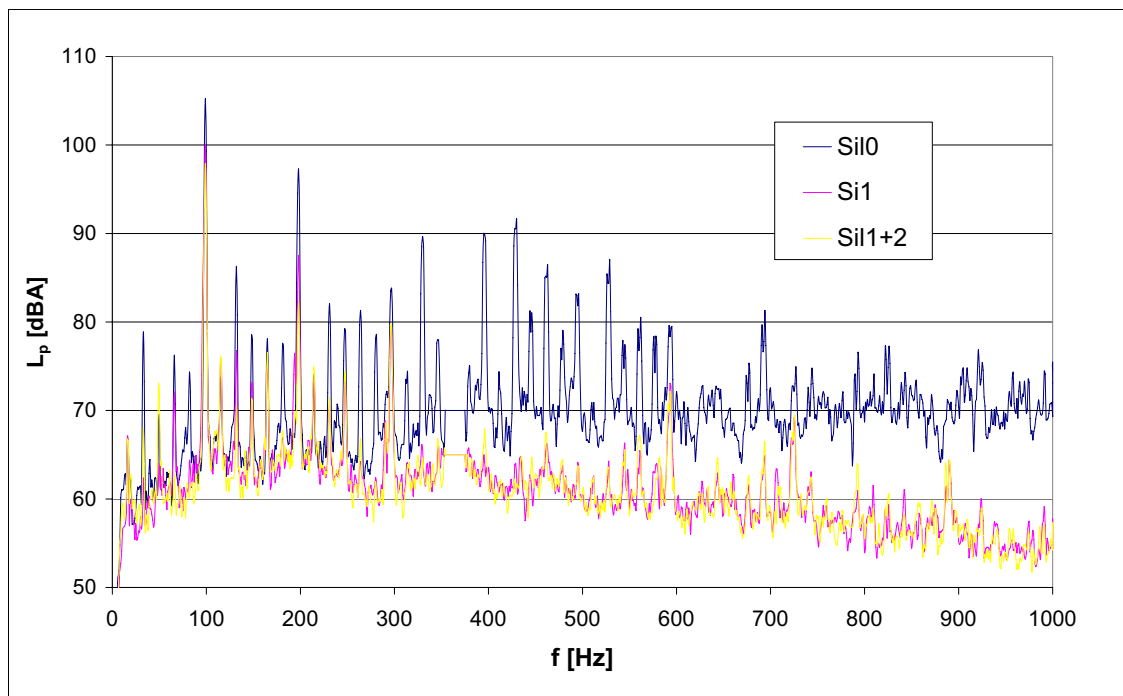


Figure 3.1: Measured pressure level, L_p , with FFT filter in frequency interval 0-1000 Hz and bandwidth 1 Hz. System Sil0, Sil1 and Sil1+2. 1.5 m from the orifice with engine in lifting mode.

that this was an external source emanating from the truck’s hydraulics. This anomaly is further addressed in the next chapter. As in chapter 2.2.4 when there was a small difference in sound pressure level for different radii (distance from the orifice), as the case was here. The 363 Hz peaks from all three settings are very similar to each other and this does not follow the pattern for internal sources.

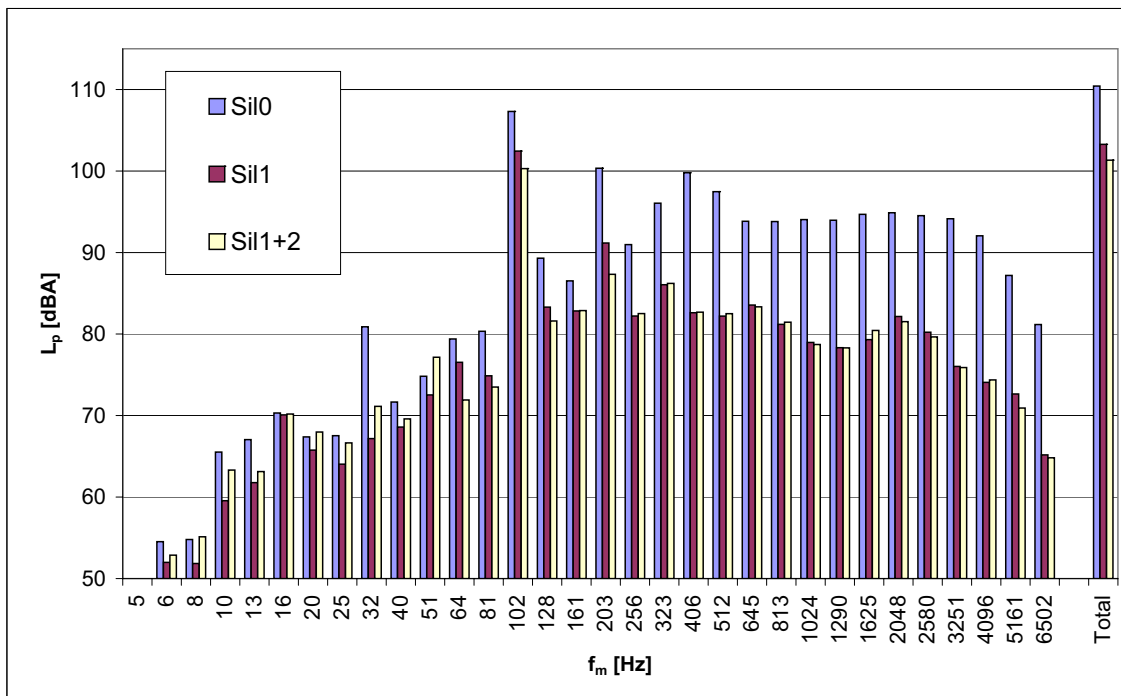


Figure 3.2: Measured pressure level, L_p , with third octave band filter. The distance is 1.5 m from the orifice and the engine is in lifting mode.

Fast Fourier transform (FFT) graphs with 1 Hz bandwidth have benefits because they illustrate with high resolution how the sound is behaving. On its drawback, the FFT-graph often becomes too complex making it difficult to compare between different mufflers and especially hard when comparing a muffler to a SIDLAB simulation. This is why, at many times, it is more convenient to make broader bands which are smoother and more easy to compare. In figure 3.2, broader bands are introduced with the width of third octave bands. Still dominant in these bands are the five peaks from before but here, however, represented in four bands. The third octave bands are referred to as their middle frequencies. No decimals are shown. The third octave band at 406 Hz contains two of the peaks discovered prior and as a result this band is now the third highest band. The two highest FFT-peaks are represented in the two highest bands; 102 Hz and 203 Hz respectively. These bands are still the most dominant and the 102 Hz band still rises above the rest, proving to be indisputably most significant for the total sound pressure level. As an effect, the third octave bands have variable width, getting wider further up the frequency scale, the bands get higher levels as the frequency increases.

A consequence of the bands being a logarithmic sum of the sound pressure levels for each frequency in the band. This results in the bands levels, though levels for each FFT-band above 1 KHz being below 75 dB(A), are very high in third octave bands. All the way from 645 Hz to 3251 Hz the levels are similar and quite high which might make it interesting to add these to a single band. In table 3.2 the entire frequency measurement scale is divided into three bands. It can be observed that the 102 Hz (third octave) band,

with system Sil0, represents half of the entire sound pressure with its 107,3 dBA. It is therefore important to work on lowering all these parts when constructing a muffler. It might be said that it is equally important to get rid of the 102 band as the remaining bands. This is true in a way but bear in mind that the 102 third octave band is so very small in bandwidth, with an even smaller peak in it, that it becomes a very isolated and well defined problem compared to the entire frequency range and that is why the 102 band is so very important. In table 3.2 the bands from 0 to 81 Hz only represent 86 dBA and is therefore too low in lift mode to be significant when constructing a muffler.

Band (f_m)	5 – 81	102	128 – 512	645 – 6502	Sum without 102-band	Sum Total
L_p [dBA]	86.0	107.3	105.1	103.7	107.5	110.4

Table 3.2: System without silencer, Sil0. Sound pressure level, L_p , for the logarithmic sum of middle frequencies 5 – 81, 102, 128 – 512 and 645 – 6502. But also the sum of all these middle frequencies, with and without the 102 third octave band are presented.

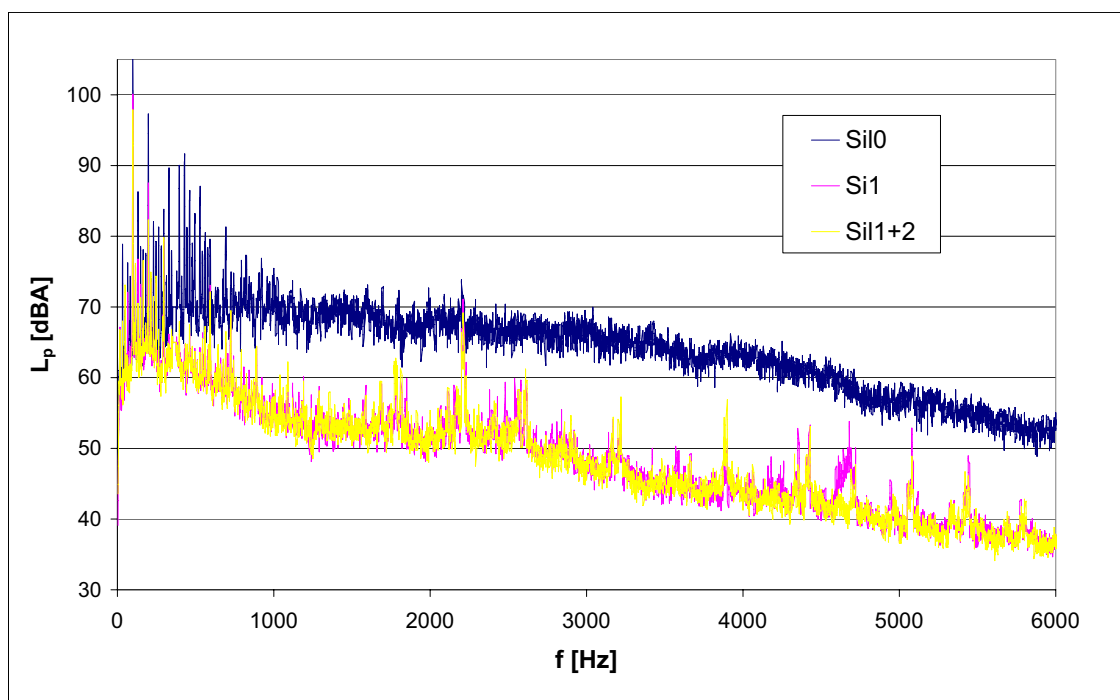


Figure 3.3: Measured pressure level, L_p , with FFT filter in frequency interval 0-6000 Hz, at a distance 1.5 m from the orifice and the engine in lifting mode.

3.2.2 Silencer 1, Sil1

Figure 3.3 shows that Sil1 absorbs sound fairly even above 1 KHz by approximately 20 dB with a few exceptions. At 2210 Hz, for example, the pressure levels are almost unchanged. This peak is rather low and far up in the frequency scale and therefore it is left as is, because its influence is too small to take into account. It might also be an external source, as it resembles the behavior of the 363 Hz peak. It is, concerning mathematical modelling, far more interesting to study sound below 1 KHz. It is more interesting mainly due to the fact that the mathematics become much easier to solve when dealing with sound in the plane wave region. Also, although the part above 1 KHz has a large influence on the

combined sound level, the Sil1 is working in a good and broadband manner here without any high peaks. This renders further analysis abundant. A quick glance of figure 3.1 at Sil0 and Sil1 shows an insertion loss of approximately 15 dB at 1 KHz down to almost 0 dB, not counting the peaks, where the functions meet just below 300 Hz. On this basis it appears that the performance of Sil1 leaves much to be desired below 300 Hz.

At a closer view the levels in $400 \text{ Hz} \geq f \geq 600 \text{ Hz}$ reveals that Sil1 erased almost all peaks here. Above 600 Hz some peaks are still visible but not nearly as high or well defined after the action of Sil1. The third octave bands in figure 3.4 shows that the insertion loss for each band is below 10 dB for $51 \text{ Hz} \geq f_m \geq 323 \text{ Hz}$. The two highest and thus most interesting peaks in the interval are 99 Hz and 198 Hz (note that $198 = 2 \times 99$). Both peaks are attenuated by Sil1 though not sufficiently. The 198 Hz peak is in the 203 Hz third octave band and is circumstantially well attenuated with its 98 dB but it is interesting seeing that the 203 band sound level are still very high.

For future considerations it should be emphasised that the 99 Hz peak (or the 102 band) stands out like a sore toe because it is so very much higher than everything which makes it the most dominating peak and that the silencers do not give it enough attention.

It is worth mentioning that if an effort is put in reducing 100 Hz then, depending on which measures are used in doing so, 300 Hz, 500 Hz and so on will also be positively affected [2]. The reduction of sound is dependent on when odd multiples of quarter wave length is in accordance with the length of the resonator. This is true for quarter wave resonators as well as for expansion chambers. This further emphasised the need to direct attention towards 100 Hz. There is a drawback to all this which is that even multiples of quarter wavelength will increase in sound pressure. In total Sil1 have an insertion loss at about 7 dBA in the system.

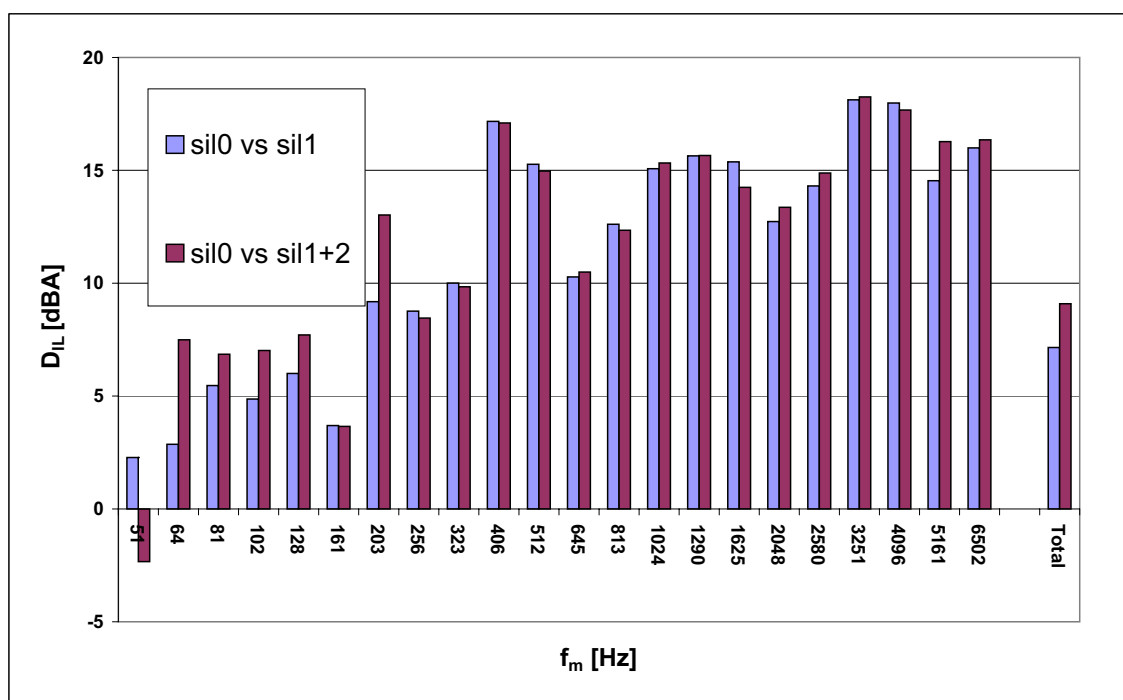


Figure 3.4: Measured insertion loss, D_{IL} , with third octave band filter in the f_m interval 51-6502 Hz. At a distance of 1.5 m from the orifice with the engine in lifting mode.

f[Hz] (f_m)	99 (102)	198 (203)	330 (323)	395 (406)	430 (406)	Total
L_p [dBA]	100	88	66	65	62	101
insertion loss	5	9	24	25	30	5

Table 3.3: The 5 most important Sound Pressure Level, L_p , peaks for Sil1. The peaks are being positioned into the middle frequency in parentheses. Their total L_p to the right. Insertion loss between Sil1 and Sil0 at the bottom.

f_m	102	203	323	406	L_p Sum
L_p [dBA] with Sil1	102.4	91.2	86.1	82.6	103.3
L_p [dBA] with Sil1+2	100.3	87.3	86.2	82.7	101.3
difference	2.1	3.9	-0.1	-0.1	2

Table 3.4: Comparison of Sil1 and Sil1+2. Sound pressure level, L_p , for the middle frequencies on the most significant third octave band.

f	99	198	297
L_p [dBA] with Sil1	100	87.5	79.5
L_p [dBA] with Sil1+2	97.9	82.3	79.8
difference	2.1	5.2	-0.3

Table 3.5: Comparison of Sil1 and Sil1+2. Sound pressure level, L_p , for the most significant frequency tops in the FFT-graph.

3.2.3 Silencer 2, Sil2

At first sight, when looking at the FFT-graph in figure 3.1 and 3.3, there is not such a big difference between Sil1 and Sil2. However, there are roughly three important peaks left when Sil1 has operated on the sound. Also the numbers in table 3.5 indicate that Sil2 is slightly more efficient on the highest peaks. Even if the figure 3.1 shows little difference compared to Sil1, it is still important to study the third octave bands. There are a few interesting results in table 3.4 and to be seen among those are that the middle frequencies, 102 and 203 bands are fairly attenuated. An assumption which could be made is that wool around a perforated pipe will attenuate frequencies above 200 Hz very well, but in this case Sil2 hardly reduces the sound at all. This does not necessarily mean that the assumption is wrong but after Sil1 has reduced the peaks, it might have rendered the data insufficient because of dominating background noise. There is some attenuating made by Sil2, but also some increase of the sound pressure level. Consequently Sil2 is counteracting itself, even though it is not particularly big attenuations in either way. In the end, the total result gives us some insertion loss. This phenomenon is clearer at low frequencies, specially the 51 and 64 bands. At the 64 band Sil2 muffle from about 76 dBA to 72 dBA, it might even be considered as good insertion loss. However, this is counteracted by middle frequency 51 Hz which is increased from about 72 to 76 dBA. In total Sil2 have an insertion loss at about 2 dBA in the system.

3.2.4 Silencer 1+2, Sil1+2

What was said in chapter 3.2.2 about Sil1 and in 3.2.3 about Sil2 combined leads us to this chapter concerning Sil1+2. Summarised it can be said that over the entire frequency interval there is a total constant insertion loss with Sil1+2, however, not as efficient as wished on 100 and 200 Hz. But the system Sil1+2 has a total insertion loss of 9,1 dBA, and the sound pressure level goes from 110,4 dBA with Sil0 to 101,3 dBA with Sil1+2, as observed in table 3.2 and 3.5. In total Sil1+2 have an insertion loss at about 9 dBA in the system.

3.3 Concluding words of the analysis

3.3.1 Summary

The first data to be analysed were from the system without silencer, Sil0. Here the dominating peaks and bands were identified. The 100 Hz and 200 Hz peaks, which the engine produce at slightly less than 2000 rotations per minute, are significantly higher than the rest of the frequencies and are for that reason causing a very great part of the noise. Due to this, most of the analysis was devoted to the region around the 100 and 200 Hz peaks. When studying the effects from Sil1 on the 100 and 200 Hz peaks it was found that the insertion loss was relatively insufficient. There exists insertion loss, but not sufficiently enough. The insertion loss for Sil1 is much more efficient on higher frequencies, just over 400 Hz and higher. Sil1 has, especially in the interval 400-600 Hz, done an enormous amount of work. The silencer Sil2 muffle the low frequencies somewhat, but does not muffle the high frequencies considerably. These are results that are quite the contrary from what was expected prior to measurements, since an assumption was that Sil2 would be most efficient at high frequencies. External peaks were identified and among those it was 363 Hz that disturbed the measuring results the most. This was also the only spot where the data was manipulated, since a mean value was generated for the entire 363 Hz peak. In the end Sil1+2 has got the highest insertion loss at about 9 dBA and Sil1 only 2 dBA lower with a total insertion loss of 7 dBA.

3.3.2 Comments

The graphs have been made in a way that it becomes easy to analyse and draw conclusions from the data. This was achieved by using bands and filters such as the third octave band filter. Disturbances in form of turbulence have been avoided when possible as in the case with the replacement pipe, used in Sil0, which was made with long smooth bends with no sudden area changes.

An important peak, 363 Hz, that was not attenuated by Sil1 or Sil2 was an external sound source. This particular source was the lifting hydraulics which have two pumps, this peak being the result of one of them. The peak also has a multiple at the double frequency but was much weaker and was therefore left alone. The second pump, expected to produce sound at 400 Hz, was absent in the graphs. Possible reasons for this might be that it is situated on the truck in such a manner that the microphones would not record the noise or that the pump quite simply did not make enough noise compared to the rest of the truck. An obvious question is if there are other peaks that emanate from an external source. More important, perhaps, is whether these possible external sources corrupt the rest of the measurements. Other frequencies likely to be external are 100 Hz, 200 Hz and 2210 Hz. The last one is addressed in chapter 3.2.2. The other two are more delicate since they represent the most important peaks as far as sound levels are concerned. No measures were taken against these frequencies because it was assumed that the main part of the sound came from the exhaust anyway. To achieve more accurate measurements it is suggested that future measurements include shielding the truck in order to make sure that only exhaust noise is recorded by the microphones. Another option is to measure at the same points as before but directing the exhaust noise to somewhere else. This way it may be assumed that the noise recorded is only background noise which can be deducted from the measurements. A third option is to place microphones to record on different locations on the truck, thus establishing which peaks are to be considered to be external sources. Identifying the peaks so to speak.

The raw data was very time consuming to work with in the beginning, but the effort of arranging the data into a massive excel-file in an easy-to-grasp fashion made the final workload on making graphs and translating data into bands much shorter. Now changes, new calculations and new analysis can be done quick and easy.

3.3.3 Sources of error in measurement

- Data are not reliable when pressure amplitudes are too small, which depends on that the background noise could be dominating in those frequencies.
- With high certainty there are even more background noise at low frequencies than for high frequencies. This statement comes from that sound with low frequencies bends around objects better than high frequencies.
- Turbulence sources in silencer system. Jaggedness in pipes, transitions between pipes, the flex pipe and pipes with bends are things that could produce high frequency noise.
- Leakage coming from flex pipe and/or transitions.

4 Acoustic theory of modelling a silencer

This chapter describes the basics of the theory behind SIDLAB. It starts with the wave equation, and then the wave equation is modified to work in one dimension. The building blocks in SIDLAB(1-port, 2-port and node) are introduced and a method is shown in which an arbitrary network may be constructed and calculated. Finally an example of how to construct a 2-port is shown.

The chapter 4.1 follow [2]. And chapter 4.2, 4.3 and 4.4 follows [7]. The example in chapter 4.5 follow [6].

4.1 The wave equation in one dimension

The wave equation is fundamental to acoustic theory. It can be applied to sound in ducts by using volume flow and mean flow velocity. In a pipe with mean flow velocity U the particle velocity vector \vec{u} may be formulated as

$$\vec{u}(\vec{r}, t) = (U + u_x)\vec{e}_x + u_y\vec{e}_y + u_z\vec{e}_z, \quad (4.1)$$

where we assume a constant velocity, U , of the mean flow over the cross section. u_x , u_y and u_z are the particle velocity in respective directions, t is time and \vec{r} the spatial vector. If we add p pressure, the linear continuity equation is

$$\frac{\partial \rho}{\partial t} + U \frac{\partial \rho}{\partial x} + \rho_0 \nabla \cdot \vec{u} = 0, \quad (4.2)$$

where the total density is $\rho_t = \rho_0 + \rho$ with ρ_0 being the density of the undisturbed medium and ρ the disturbance in the density. In a corresponding way the linear continuity equation turn into

$$\rho_0 \left(\frac{\partial \vec{u}}{\partial t} + U \frac{\partial \vec{u}}{\partial x} \right) + \nabla p = 0, \quad (4.3)$$

where the nabla operator, in a cartesian system, equals $(\partial/\partial x, \partial/\partial y, \partial/\partial z)$. When combining (4.2) and (4.3) the general wave equation takes form and becomes

$$\nabla^2 p - \frac{1}{c^2} \left(\frac{\partial}{\partial t} + U \frac{\partial}{\partial x} \right)^2 p = 0, \quad (4.4)$$

where the particle velocity vector \vec{u} is calculated via

$$\rho_0 \frac{\partial \vec{u}}{\partial t} = -\nabla p. \quad (4.5)$$

4.2 One dimension

For one dimension the wave equation becomes

$$\frac{\partial^2 p}{\partial x^2} - \frac{1}{c^2} \left(\frac{\partial}{\partial t} + U \frac{\partial}{\partial x} \right)^2 p = 0, \quad (4.6)$$

and equation 4.5 may be written as

$$\rho_0 \frac{\partial \vec{u}}{\partial t} = -\frac{\partial p}{\partial x}. \quad (4.7)$$

SIDLAB is based on the assumption that only plane waves can propagate and that they are limited to one dimension. This means that the sound waves only exist on one coordinate

that is the direction of the pipe, be it bent or straight. The travelling sound wave may then be described as

$$p = p_+ e^{i\omega t - ikx} + p_- e^{i\omega t + ikx}, \quad (4.8)$$

where p is the sound pressure and p_+ and p_- the travelling sound pressure amplitudes in a positive respectively negative direction of x . The equation is true when the perturbations in the fluids are small i.e. sound pressure level beneath 130-150 dB. Local exceptions to these demands of linearity and dimensionality can be made locally inside a 2-port. Furthermore $\omega = 2\pi f$ and $k_{\pm} = \omega/(c \pm U)$, f being the frequency, c the speed of sound in the medium and U the mean flow velocity of the medium. The plane wave assumption means that the simulations are restricted to only lower frequencies although when dealing with mufflers for vehicles this is not a problem because high frequencies are relatively easy to attack through insulation.

4.3 Ports and nodes

4.3.1 2-port

Elements such as pipes, resonators or area changes are in SIDLAB represented as 2-ports, meaning that each element has two ports (for example a pipe that is connected at each end) with possible interaction with a network. The two ports are called the inlet port and the outlet port, indicating the direction in which each port is connected. The 2-port also has two state variables described by travelling pressure amplitudes [3], illustrated with figure 4.1. Here, x_1 and x_2 are positive in the direction towards the 2-port. By using (4.8) the

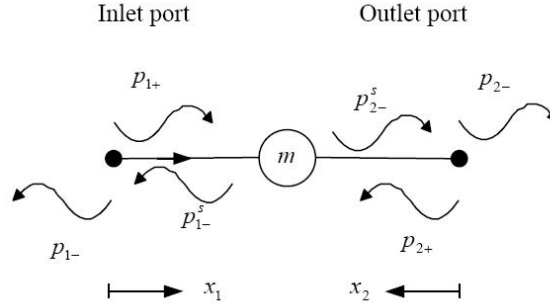


Figure 4.1: Illustration of pressure amplitudes travelling to and from a 2-port.

2-port is described mathematically by

$$\begin{pmatrix} p_{1-} \\ p_{2-} \end{pmatrix} = \mathbf{S}_m \begin{pmatrix} p_{1+} \\ p_{2+} \end{pmatrix} + \begin{pmatrix} p_{1-}^s \\ p_{2-}^s \end{pmatrix}, \quad (4.9)$$

where the outgoing p_{1-} , p_{2-} and ingoing p_{1+} , p_{2+} are travelling pressure amplitudes and also passive and unknown variables. The term, p_{1-}^s and p_{2-}^s are source pressure amplitudes going away from the 2-port and are active and known variables. The \mathbf{S}_m matrix describes how the pressure amplitudes are scattered in the 2-port m , i.e., the amounts passing through and reflected. The scattering matrix, \mathbf{S}_m , can be calculated through the reflection coefficient and transmission coefficient [5] of the 2-port.

4.3.2 1-port

The 1-port, as its name implies, has only one port and thus only affects a network through that single port. A 1-port is a representation of an element such as an engine or an exhaust. Similar to the 2-port, the 1-port is described by two state variables but they are pressure p and volume flow q in this case. The pressure p^n at the node (defined in chapter (4.3.3)) connected to the 1-port is described using two different models [3] by

$$p^n = p_0^{ns} - q^n Z^{ns} \quad (4.10)$$

and

$$p^n = Z^{ns} (q_o^{ns} - q^n) \quad (4.11)$$

where the p_0^{ns} is the constant pressure source (the active part of a 1-port), Z^{ns} the source acoustic impedance and q^n the volume flow. A combination of (4.10) and (4.11) produces the equation

$$p_0^{ns} = Z^{ns} q^{ns}. \quad (4.12)$$

The 1-port has one passive part which is permanent and one active part which is optional. In this way one may calculate a network's passive part and later add any active component, e.g. different engines connected to a single muffler since the theory is linear.

4.3.3 Node

A node is a connection point in a network to which an arbitrary number of 1-ports and 2-ports may be connected. All the nodes in a network also have one 1-port each which is always connected. It can be chosen to affect the network as detailed in chapter 4.3.2, or it can be set to have no effect on the network. In Figure 4.2 you can see four nodes in a network. A node in a network like this manages how the flow is divided between the 2-ports connected to the node. The inlet ports to a node are assumed to have the same combined area as the outlet ports. To describe a node the volume flow q is defined by [7]

$$q = \frac{p_+ - p_-}{Z}, \quad (4.13)$$

is studied. The characteristic impedance is $Z = \rho_0 c / A$, where c the speed of light and A is the cross section area where the plane wave propagates. The sum of the volume flow of all connections to a node is equal to the total volume flow of the node and can be written as

$$q^n = \sum_{m_n} \frac{p_{m_n+}^n - p_{m_n-}^n}{Z_{m_n}^n}, \quad (4.14)$$

where $Z_{m_n}^n = \rho_0 c / A_{m_n}^n$ and $A_{m_n}^n$ is the cross sectional area of the 2-port number m connected to node n . Now (4.10) can be combined with (4.14) producing

$$\frac{p_0^{ns} - p^n}{Z^{ns}} = \sum_{m_n} \frac{p_{m_n+}^n - p_{m_n-}^n}{Z_{m_n}^n}. \quad (4.15)$$

The pressure is assumed to be continuous across the node giving

$$p_{m_n+}^n + p_{m_n-}^n = p^n, \quad \forall n \text{ and } \forall m_n, \quad (4.16)$$

which together with (4.12) and (4.15) gives

$$\frac{p_0^{ns} - p^n}{Z^{ns}} = \frac{Z^{ns} q_0^{ns} - (p_{m_n+}^n + p_{m_n-}^n)}{Z^{ns}} = q_0^{ns} - \frac{(p_{1+}^n + p_{1-}^n)}{Z^{ns}}. \quad (4.17)$$

By combining (4.17) and (4.15) we get

$$q_0^{ns} - \frac{(p_{1+}^n + p_{1-}^n)}{Z^{ns}} = \sum_{m_n} \frac{p_{m_n+}^n - p_{m_n-}^n}{Z_{m_n}^n}, \quad (4.18)$$

which in matrix form becomes $\mathbf{S}_+^n \mathbf{p}_+^n = \mathbf{S}_-^n \mathbf{p}_-^n + \mathbf{q}_0^{ns}$. Here \mathbf{S}_+^n and \mathbf{S}_-^n [$m_n \times m_n$] are the positive and negative scattering matrices, respectively, for the node n , given by

$$\mathbf{S}_+^n = \begin{bmatrix} \frac{1}{Z_1^n} + \frac{1}{Z^{ns}} & \frac{1}{Z_2^n} & \cdot & \frac{1}{Z_{m_n}^n} \\ 1 & -1 & 0 & \cdot & 0 \\ 0 & 1 & -1 & 0 & \cdot \\ \cdot & \cdot & \cdot & \cdot & 0 \\ 0 & \cdot & \cdot & 1 & -1 \end{bmatrix}, \quad \mathbf{S}_-^n = \begin{bmatrix} \frac{1}{Z_1^n} - \frac{1}{Z^{ns}} & \frac{1}{Z_2^n} & \cdot & \frac{1}{Z_{m_n}^n} \\ -1 & 1 & 0 & \cdot & 0 \\ 0 & -1 & 1 & 0 & \cdot \\ \cdot & \cdot & \cdot & \cdot & 0 \\ 0 & \cdot & \cdot & -1 & 1 \end{bmatrix}. \quad (4.19)$$

\mathbf{p}_+^n and \mathbf{p}_-^n [$m_n \times 1$] are travelling pressure amplitudes going into and out from node n and \mathbf{q}_0^{ns} [$m_n \times 1$] the source strength from the 1-port connected to the node. This is a description of how the impedance affects the node and how the pressure amplitudes are scattered but also how a 1-port affects the node and subsequently the entire network. Now, we have a description of all the different components of the network but still need a description of how to connect everything.

4.4 Complete network

A representation of the entire network and how it is connected is vital for further calculation. First all the 2-ports and pressure amplitudes are written in matrix form. The pressure amplitudes for the 2-ports becomes $\mathbf{p}_\pm^c = ((p_{1\pm} \ p_{2\pm})_1 \cdots (p_{1\pm} \ p_{2\pm})_M)^T$, a [$2M \times 1$] matrix and similarly $\mathbf{p}_\pm^{cs} = ((p_{1\pm}^s \ p_{2\pm}^s)_1 \cdots (p_{1\pm}^s \ p_{2\pm}^s)_M)^T$. The c denotes that the vectors are for the complete network and s denotes that it is the source strength in the 2-port. The cs thus indicates that it is the source strength for the complete network. Left to construct are the scattering matrices for the 2-ports which are simply the diagonal elements of a [$2M \times 2M$] matrix called \mathbf{S}^c . With these, equation (4.9) becomes

$$\mathbf{p}_-^c = \mathbf{S}^c \mathbf{p}_+^c + \mathbf{p}_-^{cs}, \quad (4.20)$$

which describes how the pressure amplitudes are related in the complete network.

4.4.1 The Projection matrix

To be able to connect the 2-ports to each other through nodes we introduce the "projection matrix" \mathbb{P}^n [$m_n \times 2M$]. \mathbb{P}^n contains information as to whether node n is connected or not connected to a 2-port. The information in \mathbb{P}^n also tells whether it is an outlet or inlet port. To sum up, \mathbb{P}^n describes the connection between local pressure amplitudes and pressure amplitudes for the complete network. The matrix \mathbb{P}^n should satisfy

$$\mathbf{p}_\pm^n = \mathbb{P}^n \mathbf{p}_\pm^c,$$

where the value of \mathbb{P}^n in every position is 0 or 1, 1 if the node is connected to the 2-port, otherwise 0. Figure 4.2 describes a network of 2-ports and nodes.

For node 3 in figure 4.2 we have

$$\mathbf{p}_-^3 = \begin{pmatrix} p_{2,2-} \\ p_{1,4-} \\ p_{2,5-} \end{pmatrix}, \quad \mathbf{p}_+^3 = \begin{pmatrix} p_{2,2+} \\ p_{1,4+} \\ p_{2,5+} \end{pmatrix}.$$

where the first number in the index is 1 if the connection is an inlet port and 2 if it is an outlet port. The second number describes to which 2-port the connection goes. For example $p_{2,5+}$ is a pressure amplitude from the node(+), through an outlet port(2) and connected to 2-port 5. Now we can formulate our projection matrix \mathbb{P}^3 [3×10] as follows

$$\mathbb{P}^3 = \begin{array}{ccccccccc} \left[\begin{array}{cccccccccc} 0 & 0 & 0 & 1 & 0 & 0 & 0 & 0 & 0 & 0 \\ 0 & 0 & 0 & 0 & 0 & 0 & 1 & 0 & 0 & 0 \\ 0 & 0 & 0 & 0 & 0 & 0 & 0 & 0 & 0 & 1 \end{array} \right] & \begin{array}{l} \leftarrow \text{2-port number 2} \\ \leftarrow \text{2-port number 4} \\ \leftarrow \text{2-port number 5} \\ \leftarrow \text{Inlet port for the 2-ports 1 to 5} \\ \leftarrow \text{Outlet port for the 2-ports 1 to 5.} \end{array} \\ \begin{array}{cccccc} \uparrow & & \uparrow & & \uparrow & & \uparrow & & \uparrow & \\ & \uparrow & & \uparrow & & \uparrow & & \uparrow & & \end{array} \end{array}$$

Going back to the general description; $\mathbf{S}_+^n \mathbf{p}_+^n = \mathbf{S}_-^n \mathbf{p}_-^n + \mathbf{q}_0^{ns}$ could be rewritten to incorporate \mathbb{P}^n , it follows that:

$$\mathbf{S}_+^n \mathbb{P}^n \mathbf{p}_+^c = \mathbf{S}_-^n \mathbb{P}^n \mathbf{p}_-^c + \mathbf{q}_0^{ns}.$$

Using equation (4.20) and simplifying the expression, an equation for all nodes may be written as

$$\underbrace{\left[\sum_n (\mathbf{S}_+^n \mathbb{P}^n - \mathbf{S}_-^n \mathbb{P}^n \mathbf{S}^c) \right]}_{=\mathbf{A}} \mathbf{p}_+^c = \underbrace{\left[\sum_n \mathbf{S}_+^n \mathbb{P}^n \right]}_{=\mathbf{B}} \mathbf{p}_-^c + \underbrace{\sum_n \mathbf{q}_0^{ns}}_{=\mathbf{q}_0^{cs}},$$

The final state of \mathbf{A} and \mathbf{B} are derived through basic matrix calculations, although [7] provides an algorithm. Consequently,

$$\mathbf{A} \mathbf{p}_+^c = \mathbf{B} \mathbf{p}_-^c + \mathbf{q}_0^{cs}, \quad (4.21)$$

where \mathbf{A} and \mathbf{B} are two matrices of the form $[2M \times 2M]$ describing the scattering in the complete network. Every node in the network creates a row in \mathbf{A} and \mathbf{B} for each connection to a 2-port. The number of rows in \mathbf{A} and \mathbf{B} is two times the number of 2-ports in the system, that is $2M$ rows. The total source strength is \mathbf{q}_0^{cs} ($[2M \times 1]$ in vector form) for all 1-ports that are connected to the network. All rows in $\mathbf{A} \mathbf{p}_+^c = \mathbf{B} \mathbf{p}_-^c + \mathbf{q}_0^{cs}$, can be solved in the frequency plane for any frequency. Because \mathbf{A} and \mathbf{B} contains passive data from the 1-ports and 2-ports, it is possible to calculate \mathbf{A} and \mathbf{B} by knowing the geometry of the network. On the left side of equation (4.21), \mathbf{A} describes \mathbf{p}_+^c scattering in the network. On the right side, \mathbf{B} describes how \mathbf{p}_-^c is scattering in the network. To calculate \mathbf{A} and \mathbf{B} an algorithm could be useful. One algorithm involves the \mathbf{G} -matrix, which will be explained in the next chapter.

4.4.2 The \mathbf{G} -matrix

The \mathbf{G} -matrix is built up very simply with rows representing nodes and columns representing 2-ports in the network. All 2-ports and nodes in the network are represented by the matrix. The matrix element is denoted by its position $g(n, m)$ and the value in that position indicates whether there is a connection or not and if so in which direction. This

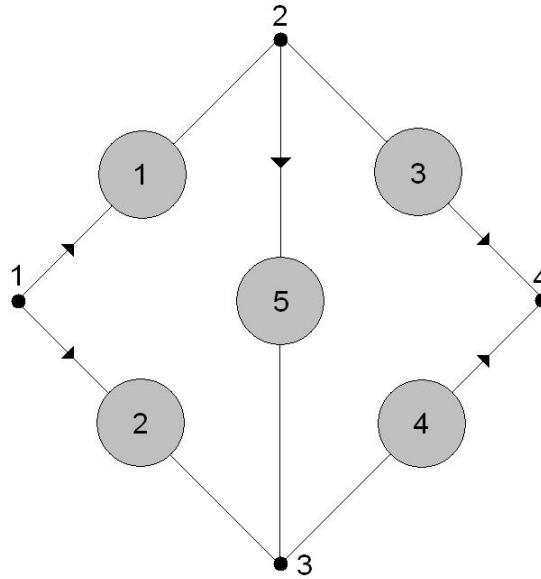


Figure 4.2: Illustration of a network containing five 2-ports, four nodes and the connections between them with directions.

is achieved by

$$g(n, m) = \begin{cases} 1, & \text{if two-port } m \text{ is connected to node } n \text{ via an inport} \\ -1, & \text{if two-port } m \text{ is connected to node } n \text{ via an outport} \\ 0, & \text{if no connection between } m \text{ and } n \text{ exists.} \end{cases}$$

Now \mathbf{A} and \mathbf{B} can be built up by studying \mathbf{G} . But first we introduce three new notations: m_n , k and l . m_n is the number of values in row n in \mathbf{G} that is not equal to 0, i.e. the number of 2-ports connected to node n . Building m_n rows in both \mathbf{A} and \mathbf{B} , every row is numbered from 1 to k . Variable l is the l :th number separated from 0 in row n in \mathbf{G} . The graph matrix for figure 4.2 is

$$\mathbf{G} = \begin{array}{ccccc} \left[\begin{array}{ccccc} 1 & 1 & 0 & 0 & 0 \\ -1 & 0 & 1 & 0 & 1 \\ 0 & -1 & 0 & 1 & -1 \\ 0 & 0 & -1 & -1 & 0 \\ \uparrow & \uparrow & \uparrow & \uparrow & \uparrow \\ 1 & 2 & 3 & 4 & 5 \end{array} \right] & \begin{array}{l} \leftarrow \text{Node 1} \\ \leftarrow \text{Node 2} \\ \leftarrow \text{Node 3} \\ \leftarrow \text{Node 4} \\ \\ \leftarrow \text{2-port number.} \end{array} \end{array}$$

Each row in \mathbf{G} gives m_n values not equal to 0, and every such value occupies 2 positions in row k_n in \mathbf{A} and 2 positions in row k_n in \mathbf{B} . For every $g(n, m)$, two values: positions $a(k, 2m - 1)$ and $a(k, 2m)$ are determined for every row $k = 1, \dots, m_n$. The same method is used in \mathbf{B} . In this way both \mathbf{A} and \mathbf{B} becomes $[2M \times 2M]$ matrices. The element $g(m, n) = 0$ gives, in \mathbf{A} , $a(k, 2m - 1) = 0$ and $a(k, 2m) = 0$. Following this method the \mathbf{B} -matrix for the network in figure 4.2 is

$$\begin{array}{c} \begin{array}{cc} m=1 & m=2 & m=3 & m=4 & m=5 \\ \overbrace{2m-1 \quad 2m} & \overbrace{2m-1 \quad 2m} & \overbrace{2m-1 \quad 2m} & \overbrace{2m-1 \quad 2m} & \overbrace{2m-1 \quad 2m} \end{array} \\ \left[\begin{array}{cccccc} S_{-11}^1 & 0 & S_{-12}^1 & 0 & 0 & 0 & 0 & 0 & 0 & 0 \\ S_{-21}^1 & 0 & S_{-22}^1 & 0 & 0 & 0 & 0 & 0 & 0 & 0 \\ 0 & S_{-11}^2 & 0 & 0 & S_{-12}^2 & 0 & 0 & 0 & S_{-13}^2 & 0 \\ 0 & S_{-21}^2 & 0 & 0 & S_{-22}^2 & 0 & 0 & 0 & S_{-23}^2 & 0 \\ 0 & S_{-31}^2 & 0 & 0 & S_{-32}^2 & 0 & 0 & 0 & S_{-33}^2 & 0 \\ 0 & 0 & 0 & S_{-11}^3 & 0 & 0 & S_{-13}^2 & 0 & 0 & S_{-13}^3 \\ 0 & 0 & 0 & S_{-21}^3 & 0 & 0 & S_{-23}^2 & 0 & 0 & S_{-23}^3 \\ 0 & 0 & 0 & S_{-31}^3 & 0 & 0 & S_{-33}^2 & 0 & 0 & S_{-33}^3 \\ 0 & 0 & 0 & 0 & 0 & S_{-11}^4 & 0 & S_{-12}^4 & 0 & 0 \\ 0 & 0 & 0 & 0 & 0 & S_{-21}^4 & 0 & S_{-22}^4 & 0 & 0 \end{array} \right] \begin{array}{l} \left. \begin{array}{l} k_n = 1 \\ k_n = 2 \end{array} \right\} n = 1, m_1 = 2 \\ \left. \begin{array}{l} k_n = 1 \\ k_n = 2 \\ k_n = 3 \end{array} \right\} n = 2, m_2 = 3 \\ \left. \begin{array}{l} k_n = 1 \\ k_n = 2 \\ k_n = 3 \end{array} \right\} n = 3, m_3 = 3 \\ \left. \begin{array}{l} k_n = 1 \\ k_n = 2 \end{array} \right\} n = 4, m_4 = 2 \end{array} \end{array} \quad (4.22)$$

The unknown vector \mathbf{p}_+^c can now be solved and using (4.20), \mathbf{p}_-^c is also solved. With that, all the pressure amplitudes are now known.

4.5 Examples

4.5.1 Making an S-matrix

This example shows a general way to produce an **S**-matrix from two impedance changes, for example an expansion chamber. This formalism is based on travelling pressure waves as state vectors and a scattering matrix **S** [4].

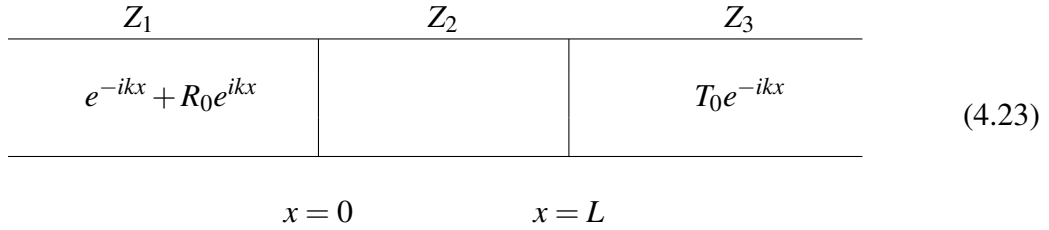


Figure 4.3: Representation of a pipe with two impedance changes at $x = 0$ and $x = L$. The incident wave e^{-ikx} and the transmitted wave T_0e^{-ikx} travel from left to right.

A wave travelling through a pipe may be described by $\mathbf{p} = p_i e^{-ikx} + p_r e^{ikx}$. Assuming $p_i = 1$, the total incident wave can be expressed as $e^{-ikx} + R_0 e^{ikx}$, when $x < 0$. Here R_0 is the reflected pressure amplitude. The wave travels in a pipe which characteristic impedance changes from Z_1 to Z_2 and finally to Z_3 , where no reflection exists in the last pipe. This let us to set the outgoing transmitted wave to $T_0 e^{-ikx}$ where $x > L$. Note that only a right-travelling wave is present in this example. Three cases a), b), and c) are set up to include all different waves in the two-port:

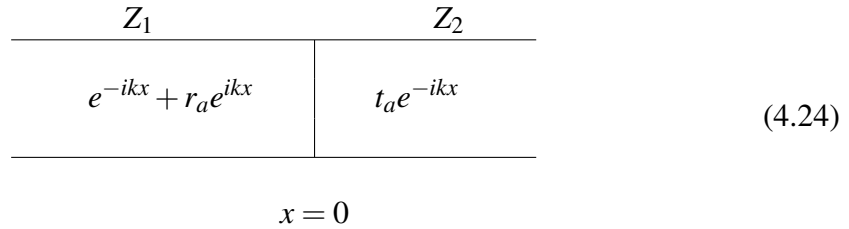


Figure 4.4: A closer look at the left side of the pipe with impedance changes at $x = 0$. The wave travels from left to right. $e^{-ikx} + r_a e^{ikx}$ is the total wave travelling from the left and at $x = 0$ the transmitted part of the wave is $t_a e^{-ikx}$.

Case a) Let $e^{-ikx} + r_a e^{ikx}$ be the wave travelling from left to right in $x < 0$ and $t_a e^{-ikx}$ the transmitted wave in $x > 0$ assuming a reflection free end; se figure 4.24. The reflection is achieved by a change in impedance from Z_1 to Z_2 at $x = 0$. Here r_a and t_a are known.

Z_1	Z_2	
$t_b e^{ikx}$	$e^{ikx} + r_b e^{-ikx}$	
$x = 0$		

(4.25)

Figure 4.5: A closer view of the left side of the pipe with impedance changes at $x = 0$. The wave e^{ikx} in $x > 0$ is impinging from right giving a reflected wave $r_b e^{-ikx}$ in $x > 0$ and a transmitted wave $t_b e^{ikx}$ in $x < 0$.

Case b) Let $e^{ikx} + r_b e^{-ikx}$ in $x > 0$ be the wave travelling from right to left and $t_b e^{ikx}$ the transmitted wave in $x < 0$; see figure 4.25. This is true when $x < 0$ and when the left side is assumed to be reflection free (for future reference, this case is equivalent to $B e^{ikx} + B r_b e^{-ikx} = B t_b e^{ikx}$). Here r_b and t_b are known.

Z_2	Z_3	
$e^{-iky} + r_c e^{iky}$	$t_c e^{-iky}$	(4.26)
$y = x - L = 0$		

Figure 4.6: A closer look at right side of the pipe with impedance changing in $y = x - L = 0$. The wave e^{-iky} in $y < 0$ is impinging from left giving a reflected wave $r_c e^{iky}$ in $y < 0$ and a transmitted wave $t_c e^{-iky}$ in $y > 0$.

Case c) Let $e^{-iky} + r_c e^{iky}$ be the travelling wave from left to right in $y < 0$ and $t_c e^{-iky}$ the transmitted wave in $y > 0$; see figure 4.26. The reflection is achieved by a change in impedance from Z_2 to Z_3 at $y = x - L = 0$. Here r_c and t_c are known.

The pressure in the entire 2-port may be described by

Z_1	Z_2	Z_3	
$e^{-ikx} + R_0 e^{ikx}$	$A e^{-ikx} + B e^{ikx}$	$T_0 e^{-ikx}$	(4.27)
$x = 0$ $x = L$			

Figure 4.7: Representation of a pipe with two impedance changes at $x = 0$ and $x = L$. The incident wave travels from left to right.

The required variables are now given and the calculations may commence. The objective is to obtain expressions for R_0 and T_0 . Starting with $x = 0$ we have

$$R_0 = r_a + B t_b,$$

where r_a represents the first reflection and is given in a), and $B t_b$ the transmission from the wave $B e^{ikx}$ and is given in b). Similarly,

$$A = t_a + B r_b,$$

describing the first transmission from the wave e^{-ikx} and reflection from $B e^{ikx}$. Here, t_a from case a) and $B r_b$ from case b). After this we would like to derive an expression for T_0 . In the middle part of (4.27) the right going wave can be rewritten as

$$A e^{-ikx} = A e^{-ikL} e^{-ik(x-L)} = A e^{-ikL} e^{-iky}.$$

From case c) we then get in the right part of (4.27) that

$$A e^{-ikL} t_c e^{-iky}, \tag{4.28}$$

which combined with T_0 gives

$$T_0 e^{-ikx} = A e^{-ikL} t_c e^{-iky} = A e^{-ikL} t_c e^{-ik(x-L)} = A t_c e^{-ikx}$$

which simplifies to

$$T_0 = A t_c.$$

Now R_0 and T_0 are expressed in the variables A and B . We want an expression of R_0 and T_0 expressed without A and B . When studying $x = L$ we can produce expressions for A and B in this point. The incident wave

$$Ae^{-ikx} = Ae^{-ikL}e^{-ik(x-L)} = Ae^{-ikL}e^{-iky}$$

produces the reflected wave

$$Ae^{-ikL}r_c e^{iky} = Ae^{-ikL}r_c e^{ik(x-L)} = Ar_c e^{-2ikL}e^{ikx}$$

on the left hand side. Thus, $B = Ar_c e^{-2ikL}$ and because $A = t_a + Br_b$ this means that

$$\frac{1}{r_c}e^{2ikL}B = t_a + Br_b$$

and

$$B = \frac{t_a}{\frac{1}{r_c}e^{2ikL} - r_b}.$$

Since $R_0 = r_a + Bt_b$ and $T_0 = At_c$ we can write the expressions in its final state:

$$R_0 = r_a + \frac{t_a t_b}{\frac{1}{r_c}e^{2ikL} - r_b}$$

or

$$p_{1-} = p_{1+} \left(r_a + \frac{t_a t_b}{\frac{1}{r_c}e^{2ikL} - r_b} \right),$$

respectively,

$$T_0 = \frac{t_a t_c}{1 - r_c r_b e^{-2ikL}}$$

or

$$p_{2-} = p_{2+} \left(\frac{t_a t_c}{1 - r_c r_b e^{-2ikL}} \right).$$

4.5.2 Expansion chamber

This theory can now be applied to an expansion chamber where the impedance changes from Z to Z_0 and back to Z again (Let $Z_1 = Z_3 = Z$ and $Z_2 = Z_0$). Writing the entire scattering matrix the different elements can be identified.

$$\begin{bmatrix} p_{1-} \\ p_{2-} \end{bmatrix} = \mathbf{S}_m \begin{bmatrix} p_{1+} \\ p_{2+} \end{bmatrix} = \begin{bmatrix} S_{11} & S_{12} \\ S_{21} & S_{22} \end{bmatrix} \begin{bmatrix} p_{1+} \\ p_{2+} \end{bmatrix}$$

Since the reflected and transmitted amplitudes are $R_0 = p_{1-}$ and $T_0 = p_{2-}$ this lets us to define two of the scattering matrix elements as $S_{11} = R_0$ and $S_{21} = T_0$. At a point of change of cross-sectional area the relationship between the reflected and incident wave is expressed [5] by

$$\frac{\mathbf{p}_r}{\mathbf{p}_i} = \frac{Z_b - Z_a}{Z_b + Z_a}, \quad (4.29)$$

where a wave leaves a pipe with impedance Z_a and enters a pipe with impedance Z_b . Three reflection coefficient exists as follows (note that the incident waves, p_i , is set to 1)

$$\left\{ \begin{array}{l} Z \rightarrow Z_0 : r_a = \frac{Z_0 - Z}{Z_0 + Z} \text{ and } t_a = r_a + 1 = \frac{2Z_0}{Z_0 + Z} \\ Z \leftarrow Z_0 : r_b = \frac{Z - Z_0}{Z_0 + Z} \text{ and } t_b = r_b + 1 = \frac{2Z}{Z_0 + Z} \\ Z_0 \rightarrow Z : r_c = \frac{Z - Z_0}{Z_0 + Z} \text{ and } t_c = r_c + 1 = \frac{2Z}{Z_0 + Z}. \end{array} \right.$$

Using this new information,

$$S_{11} = \frac{Z_0 - Z}{Z_0 + Z} + \frac{\frac{4ZZ_0}{(Z_0 + Z)^2}}{\frac{Z_0 + Z}{Z - Z_0} e^{2ikL} - \frac{Z - Z_0}{Z_0 + Z}},$$

and

$$S_{21} = \frac{4ZZ_0}{(Z_0 + Z)^2 - (Z - Z_0)^2 e^{-2ikL}}.$$

Because of the symmetry in this example, $S_{22} = S_{11}$ and $S_{21} = S_{12}$. Thus, we have a scattering matrix \mathbf{S}_m which represents an expansion chamber.

5 Modelling of silencer

This chapter contains a short background about muffler modelling followed by an example of how to interpret a physical muffler into SIDLAB code after which an explanation follows of how the Sil1 and sil2 were modelled. The results of the SIDLAB output is then compared to the experimental data analysed in chapter 3. This comparison verifies that the simulation of the silencers are accurate and corresponds to the reality. This led to the possibility to make three different suggestions to improve the existing mufflers.

5.1 Modelling background

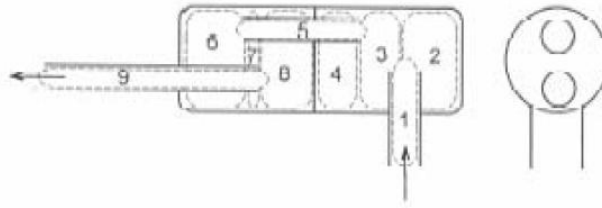
The art of simulating reality with a computer model to a great accuracy is something highly appreciated. Simulation in general is a great help in doing a minimum of expensive, time consuming testing. Depending on the tools used (and the people using these tools) the result can be more or less accurate. This thesis uses a tool designed for sound in ducts, using MATLAB as a base of calculations and is consequently called SIDLAB. SIDLAB should be considered to be a highly accurate tool when dealing with the well proven elements such as a straight pipe, an expansion chamber or a quarter wave resonator. The reality, however, does not always consist of well defined acoustic elements. Instead experience and calculations have to be used to be able to get a resemblance of the actual muffler, as is the case for the thesis. A simulation does not even have to be very accurate in order to get important information from it. A crude simulation might even be enough to get an overall image of how the muffler works and what elements or parameters that should be altered to make a good improvement. The simple fact that only a reduction of length, instead of an increase, of an element should be made has already cut testing costs in half.

Simulation requires that properties are known, some more important than others depending on frequency and accuracy of the result. The simulation variables can be tweaked in several different ways to produce similar results. The interpretations vary depending on the desired result but this occasion concerns length, volume, perforation, insulation and source impedance. A muffler is basically represented in cascade starting from the source in form of a *start node* and a source impedance, then the elements follow in the same order as the flow of sound and mean flow. To finish it all off there are several options but *free space*, with an end node, was used in this case. To obtain D_{IL} (see chapter 2.2.2) a reference must be entered. This is appropriately set to the same length as the muffler system which is to be simulated.

5.2 Example from the SIDLAB manual

To divide a volume into useful smaller elements is not trivial. This example from the SIDLAB manual will perhaps shed some light on one way to address the problem. The example will show how elements could be chosen; we do not calculate the result of the simulation. The figure 5.1 is of a so called rock drill silencer and the volumes are divided into quarter wave resonators and pipes. There are two different ways to make this division. The choice to be made is simply the way that works best but striving to keep the resonators length in the direction of propagation is a good rule to follow. In figure 5.1 this direction is right to left.

Because the pipe "element 1" enters from the side, the first quarter wave resonator is from the center of the pipe to the far right end of the silencer. The part between the center of pipe 1 to the beginning of the pipe 5 is considered to be a pipe. To the left of the beginning of pipe 5 the volume is once again considered to be a quarter wave



Element no.	Data [m, m ²]	Type
1	L=0.046, S=0.00056	Pipe
2	L=0.036, S=0.00182	Quarter-Wave
3	L=0.017, S=0.00182	Pipe
4	L=0.017, S=0.00157	Quarter-Wave
5	L=0.0664, S=0.00025	Pipe
6	L=0.034, S=0.00157	Quarter-Wave
7	L=0.006, S=0.00182	Pipe
8	L=0.025, S=0.00157	Quarter-Wave
9	L=0.11, S=0.00025	Pipe

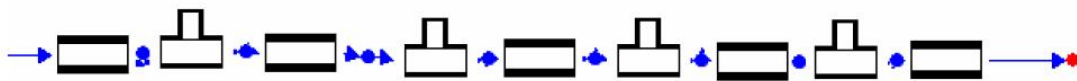


Figure 5.1: Top: Silencer for a rock drill. Middle: Data for elements in table. Below: The belonging schematic picture for all elements.

resonator. Simplified, the resonators could be thought of as volumes where no mean flow can exist. Between element 1 and 5 it is obvious that the exhaust will flow. Although not so straightforward the same theory has been applied to the volume to the left of the figure. Creating two more quarter wave resonators and one pipe out of one volume.

5.3 Modelling Sil1 and Sil1+2

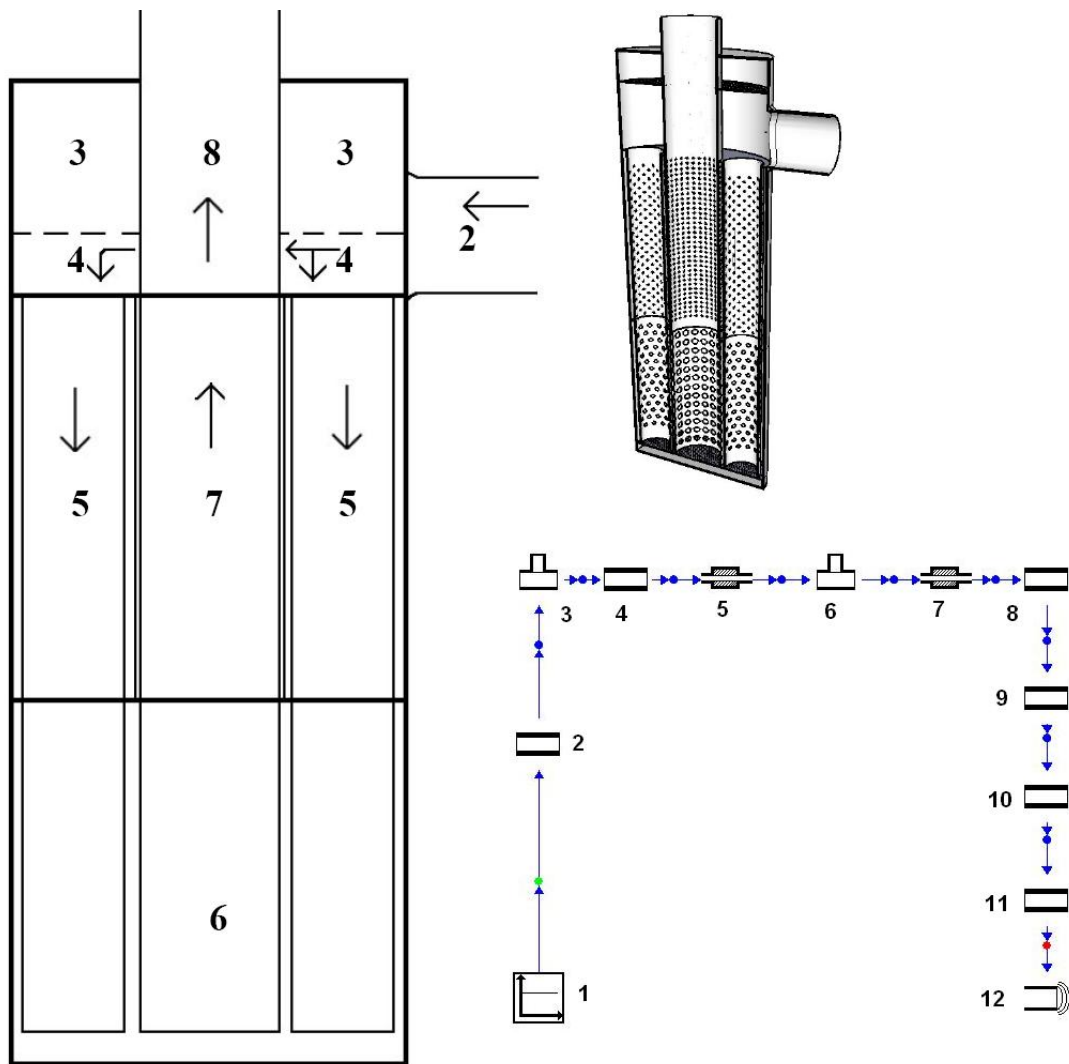


Figure 5.2: Left: Silencer 1 in 2-D. Top Right: Silencer 1 cut up in 3-D. Bottom Right: The schematic picture over all elements in system.

To the left in figure 5.2 Sil1 in 2-D can be seen, every volume has a number in this picture which represents an element in the SIDLAB scheme down to the right. Up to the right Sil1 cut up in 3-D could be studied. The volumes is numbered in the 2-D picture and also in the schematic SIDLAB picture. When dividing the silencer it is done in the same way as in chapter 5.2. All element data are displayed in table 5.1. A description of all the elements and why they are chosen follows:

1. Starting node. With the input Source impedance.
2. Pipe. This pipe represents the length between engine and silencer 1. The pipe is 0.85 m, but a length of 0.35 m has been added to it because of the engines own length between turbo and outlet from engine. Observe that this length has been estimated. Totally, this pipe-element has a length of 1.20 m.
3. Quarter wave resonator. The elements named 3 and 4 are actually one single volume. This division has been done using the same method as in the example from

Element	Type	Length (m)	A (m ²)	Pipe A (m ²)	Ch A (m ²)	FR (Pa $\frac{m^2}{m^2}$)	Axial FR	Rad FR	In A (m ²)	Out A (m ²)	Re(SI) (-)	Im(SI) (-)	Temp (°C)
1	Constant		0.00567								3	0	340
2	Pipe	1.2	0.00567			0							340
3	Quarter Wave	0.14	0.03			22000			0.00567	0.03			340
4	Pipe	0.04	0.03			0							340
5	Lined Duct	0.31		0.00704	0.03		11000	11000					330
6	Quarter Wave	0.29	0.039			10			0.00704	0.00754			330
7	Lined Duct	0.31		0.00754	0.0096		100	100					320
8	Pipe	0.18	0.00754			0							310
9	Pipe	0.85	0.00754			0							310
10	Pipe	1.4	0.00754			0							310
10	Lined Duct	1.4		0.00754	0.01886		0	0					310
11	Pipe	0.84	0.00754										310
12	Free Space		0.00754										300

Table 5.1: The data for all elements in system with Sil1 and Sil1+2.

the SIDLAB manual above. The quarter-wave resonator has the length 0.14 m and has a theoretical maximum sound reduction at around 900 Hz. The resonator consists partly of insulation which is why the sound reduction will be slightly broader, around 700-900 Hz. To simulate insulation a flow resistivity of 22 000 rayl/m² has been added to the quarter wave resonator.

4. Pipe.
5. In the silencer there are two perforated pipes in an insulated volume. The pipes are said to be coupled since the sound interacts between them. They are simulated as one pipe with the same cross section area as the two separate pipes together. To simulate insulation there has been added a flow resistivity of 11 000 rayl/m².
6. This is a complicated part of the muffler and consists of three perforated pipes with a perforated plate with insulation at the end of the volume. There are several possibilities of how to simulate this but for this model it is represented as a large quarter wave resonator of length 0.27 m and all the separate parts in the volume have been interpreted as a flow resistivity of 10 rayl/m². The theoretic sound reduction for the resonator is 450 Hz. The amount of insulation is so small in this resonator compared to the entire volume that it has been ignored and only the perforations were included in the flow resistivity.
7. This is a lined duct with a very small amount of lining.
8. Pipe. The last pipe-length in silencer 1.
9. Pipe.
10. Pipe/lined duct. This is where the additional silencer (lined duct) called Sil2 is placed. It is either a lined duct or a pipe of identical length depending on configuration.
11. Pipe.
12. Ending node. Free space.

The flow resistivity in rayl/m² is estimated for different rock wool products from information [1]. Temperature in each element are extrapolated from measured values, see appendix A.1. The thesis is not concentrated on high frequency sound and because of that the flow resistivity causing sound absorption is not that important. The results from modelling these silencers are given in next chapter, and the differences between the result from modelling and measurement are discussed.

5.4 Comparison between modelling and measurement

5.4.1 Sil1

In order to compare the measurements with the computer model it is necessary to set SIDLAB to produce insertion loss rather than transmission loss. In figure 5.3 the insertion loss from the peaks with more than 80 dB sound pressure level are shown. Additionally two peaks in the 750-1000 Hz interval, which are below 80 dB, are also in the data selection so that the entire 0-1000 Hz interval is represented.

In the 0-220 Hz interval, which is very complicated to describe in a computer model, the D_{IL} is very small in the measurement as well as in the SIDLAB calculations. In table

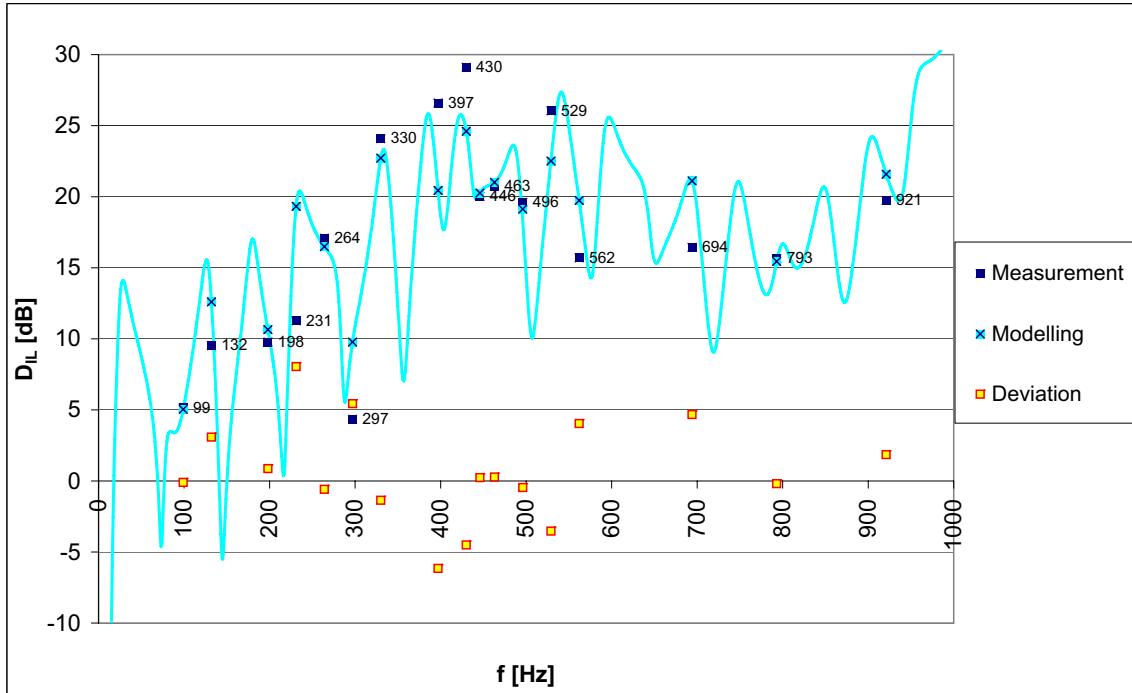


Figure 5.3: The insertion loss for 17 peaks in the measurement marked by filled squares. The simulated insertion loss function marked by x, and the deviation between measurement and modelling for Sil1 marked by empty squares. Measurement is for lifting mode, 1.5 m from orifice. The frequency range is 0-1000 Hz.

Peak	Frequency [Hz]	Sound level [dBA]	Measured D_{IL}	Modelled D_{IL}	Deviation
1	99	105	5	5	0
2	132	86	10	13	3
3	198	97	10	11	1
4	231	82	11	19	8
5	264	81	17	16	-1
6	297	84	4	10	5
7	330	90	24	23	-1
8	397	89	27	20	-6
9	430	92	29	25	-5
10	446	81	20	20	0
11	463	86	21	21	0
12	496	83	20	19	0
13	529	87	26	23	-4
14	562	80	16	20	4
15	694	81	16	21	5
16	793	77	16	15	0
17	921	77	20	22	2

Table 5.2: Insertion loss for 17 peaks in the measurement. The modelled insertion loss and the deviation between measurement and modelling for Sil1. The measurement is for lifting mode, 1.5 m from orifice. The frequency range is 0-1000 Hz.

5.2 there are three frequency points with more than 5 dB in deviation. In graph 5.3 these lie in a steep slope meaning that a slight skew of either curve (measurement or modelling) will make them fit with a much smaller deviation. However, it might also give an opposite result, i.e., a mismatch. In the 220-600 Hz interval the deviations are quite small and the modelling and measurement are very similar to each others trends. This small deviation has been achieved by assuming that a part of a volume in Sil1 is a large quarter wave resonator, *element 6*, in SIDLAB. Further up the frequency scale, from 600 Hz to 1000 Hz, there are also small deviations. The model, however, shows slightly higher D_{IL} than the measurement, but the trends remain similar. The quarter wave resonator called *element 3* is efficient at 900 Hz. Also noticeable in table 5.2 is that for most peaks the D_{IL} is higher for the modelling than for the measurements. This is assumed to be a result of disturbance of external sources.

5.4.2 Sil1+2

When modelling system Sil1+2 the silencer Sil2 has been installed onto the system Sil1. In other words to construct system Sil1+2 the pipe in *element 10* has been replaced by a lined duct. All the other elements and their variables have the same values as prior in Sil1. Viewing figure 5.4, Sil2 seems to work in a broadband and efficient manner in

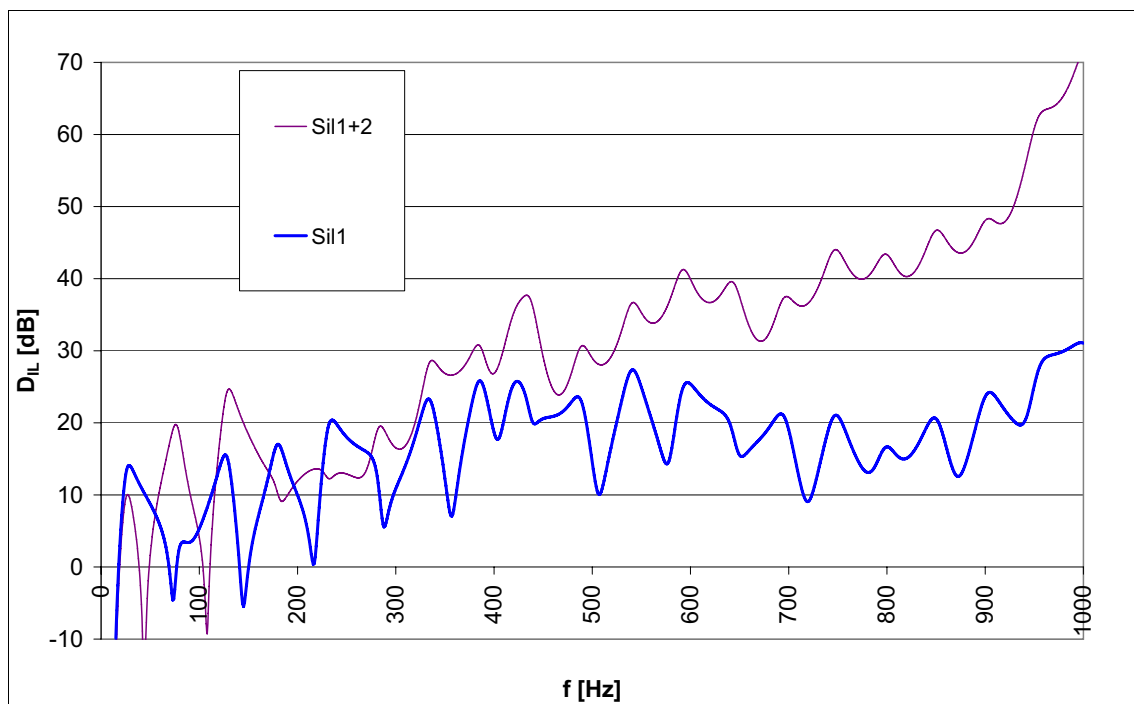


Figure 5.4: Sil1 vs Sil1+2 in modelling.

the higher frequencies, above 220 Hz. However, according to the measurement there is no attenuation in this interval. The reason, explained in chapter 3.2.3, is that Sil1 is assumed to attenuate the noise at this frequency very well and the efficiency of Sil2 is drowned in background noise. This means that the noise at high frequencies, which originates from other external sources, is higher than the noise coming from the silencer system. Looking at the interval 0-220 Hz you can see that the insertion loss is slightly better, and this corresponds to the measurement. Thus, the measurement has a little bit better insertion loss in the peaks 100 and 200 Hz as could be seen in figure 3.2 by the third octave band 102 and 203.

Figure 5.3 portrays a simulation which is very close to the measurements. It is therefore assumed that the simulation is an accurate description of the real Sil1 and Sil2 which makes it possible to make the suggested improvements in the next chapter.

5.5 Improved Sil1

There are many ways to improve a silencer. In chapter 5.5.1 it is shown two general ways to improve a silencer which are meant to determine whether the silencer is poorly dimensioned or if it is not. Chapter 5.5.2 contains a direct method of improving the insertion loss at the hard-to-get 100 Hz frequency.

5.5.1 Axial and radial increase of volume

What first comes in to mind is to try to tune the pipes so that they work better at 100 Hz and 200 Hz which is simply done by making the pipes longer. The figure 5.5 shows the effect of all lengths being doubled, giving an axial increase in volume.

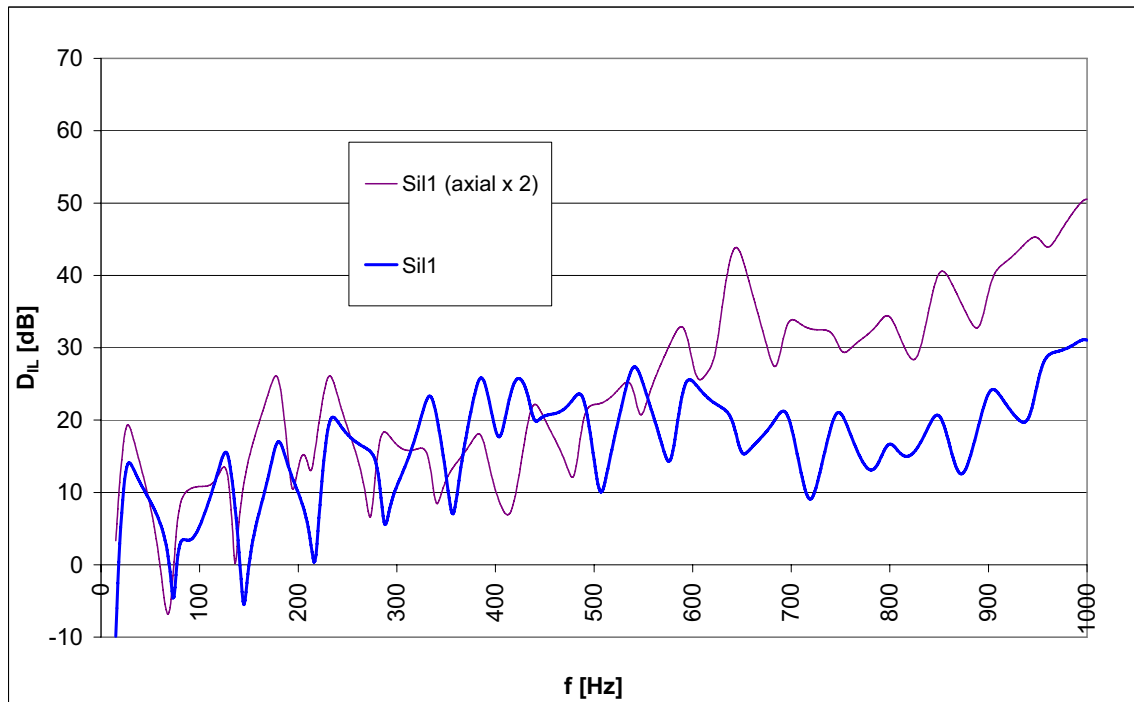


Figure 5.5: Sil1 doubled in axial length compared to Sil1.

In figure 5.5, a general displacement towards lower frequencies takes place. The 450 Hz peak is now around 225 Hz which relates to the double length of the quarter wave resonator, element 6, from chapter 5.3. To get this element to attenuate at 100 Hz more than double the length would be needed which makes it a poor option due to lack of space in the truck. Note that the muffler is now only tuned and has not a, substantial, general increase in efficiency.

An other option is to increase the radial dimensions by two, thus quadrupling the volume but keeping the original lengths of the pipes. The insertion loss seen in figure 5.6 is clearly much higher for this latter configuration. There is a broad band increase of efficiency here but for 100 and 200 Hz there is still little change. These two models strongly implies that the muffler is too small and poorly tuned as said in chapter 3.3.1.

5.5.2 Parallel resonator

It seems that other measures must be made in order to improve at the difficult low frequencies. One way is to use a parallel resonator. A parallel resonator divides the sound in two branches with different length in the same manner as a half-wave resonator[3], but

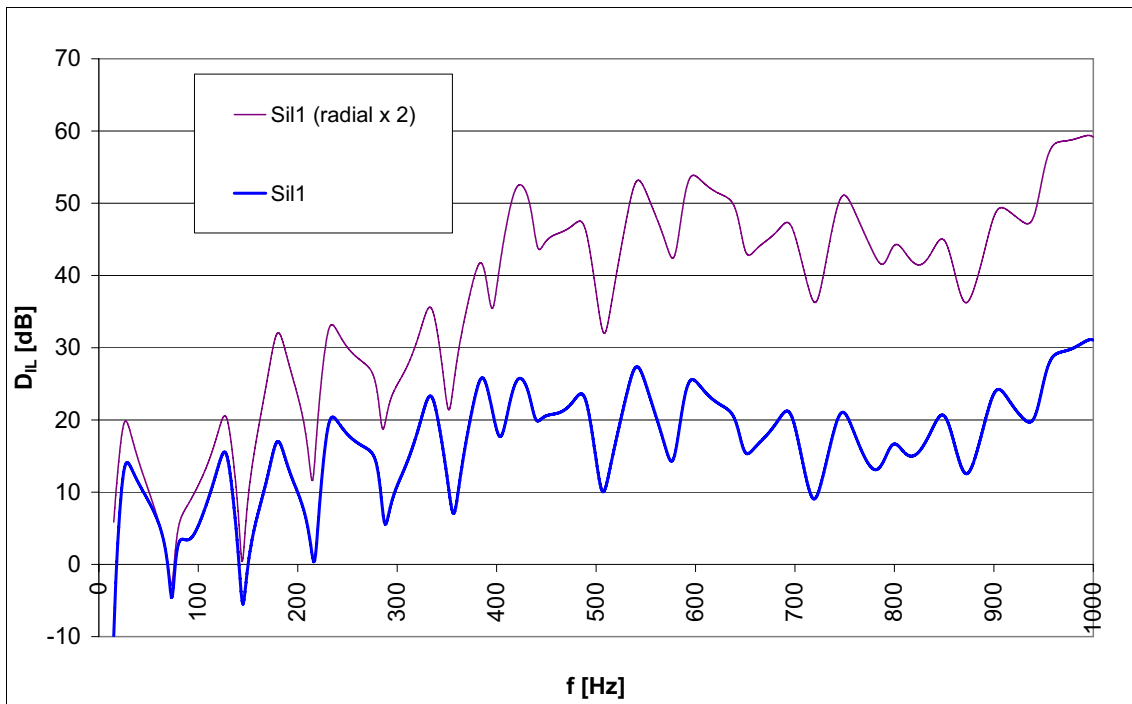


Figure 5.6: Sil1 doubled radii compared to Sil1.

also leads the sound into a volume. The two branches are combined again at an appropriate place in the muffler. With this method one can reach those hard-to-get frequencies down at 100 Hz without major alterations of the muffler dimension. The drawback of this resonator is that, due to the bypass, it leaks sound and loses insertion loss where the resonator is not tuned. This means that if the resonator is tuned for low frequencies it drops D_{IL} at higher frequencies. To tune a parallel resonator to 100 Hz a difference in distance of 1,6 m is needed and this is achieved through elongating the elements 5 and 7 with 0.5 m each. Now a leakage is needed to bypass the sound. One solution is to drill holes in element 7 as portrayed in figure 5.7, the silencer to the right.

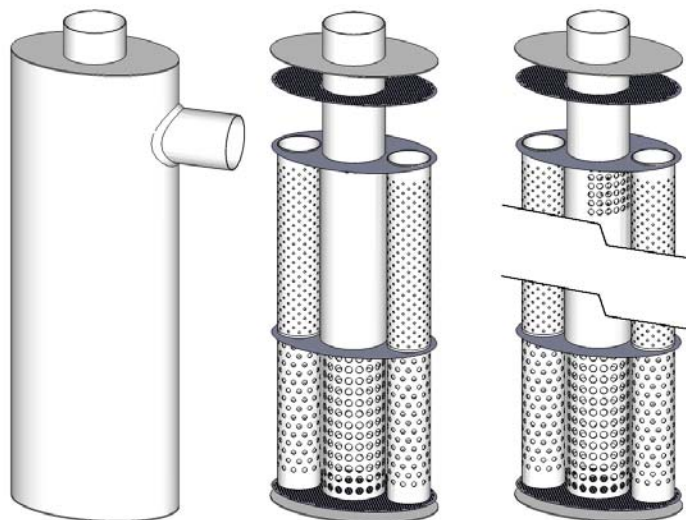


Figure 5.7: Left: Sil1. Middle: Sil1 without shell. Right: Sil1 with an example of drilled holes.

The extraordinary increase of insertion loss at 100 Hz is astonishing, although the peak is very thin as figure 5.8 shows and therefore makes the muffler unstable. At higher frequencies the D_{IL} is slightly lower at some points. It should be noted that this is not a solution at its final state but rather a way to show that 100 Hz can be attenuated with simple and inexpensive measures. Further testing and modelling is required for this idea to be ready for implementation in a truck. Because the higher frequencies lacked attenuation in the parallel resonator example, the idea came to mind to use the Sil2 in addition to the modified system, since it is designed for the high frequency range. An example of how a parallel resonator may be accomplished is portrayed in figure 5.9. This configuration has high D_{IL} in higher frequencies as well as a two high wide peaks by 100 Hz and 200 Hz.

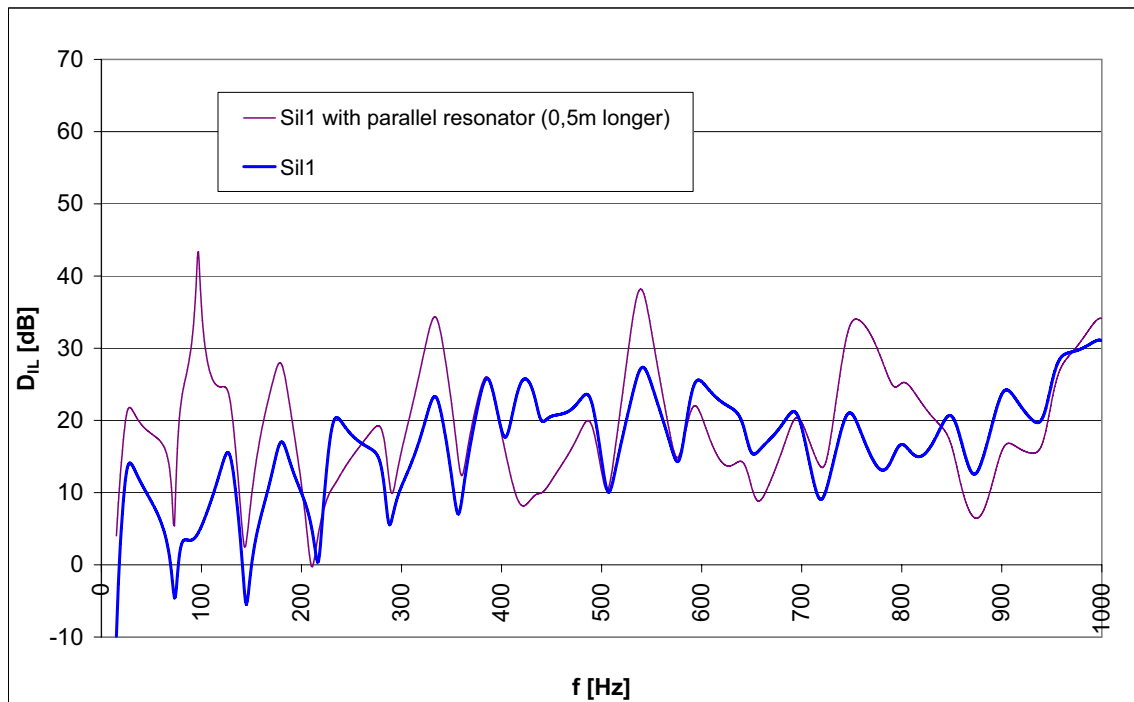


Figure 5.8: Built-in parallel resonator into silencer Sil1 in system sil1 compared to system Sil1.

5.6 Concluding words of the modelling of a silencer

5.6.1 Results

The simulations provides a proof of that the new measuring method in section 2, developed for the thesis, worked. Without this new method it is much more complicated to get the sufficient data to work with. The currently used method involves sending the engine and the complete silencer system to the Marcus Wallenberg Laboratory. The simulations also show that SIDLAB is a useful tool when developing new mufflers and when analysing existing mufflers. It may also be helpful when reducing total sound of a truck, for example, by identifying which noise that originates from the engine and noise that originates from different parts of the vehicle.

After modelling the existing Sil1 and Sil2 three improvements where proposed for Sil1. The two first alternatives show that the silencer Sil1 is poorly dimensioned; Sil1 is too small. The third alternative provides a suggestion of how to attenuate the low frequency area. The well defined peak at 100 Hz is now in reach for the silencer and the insertion loss for Sil1, with a parallel resonator implemented, increases creating an incredible result as

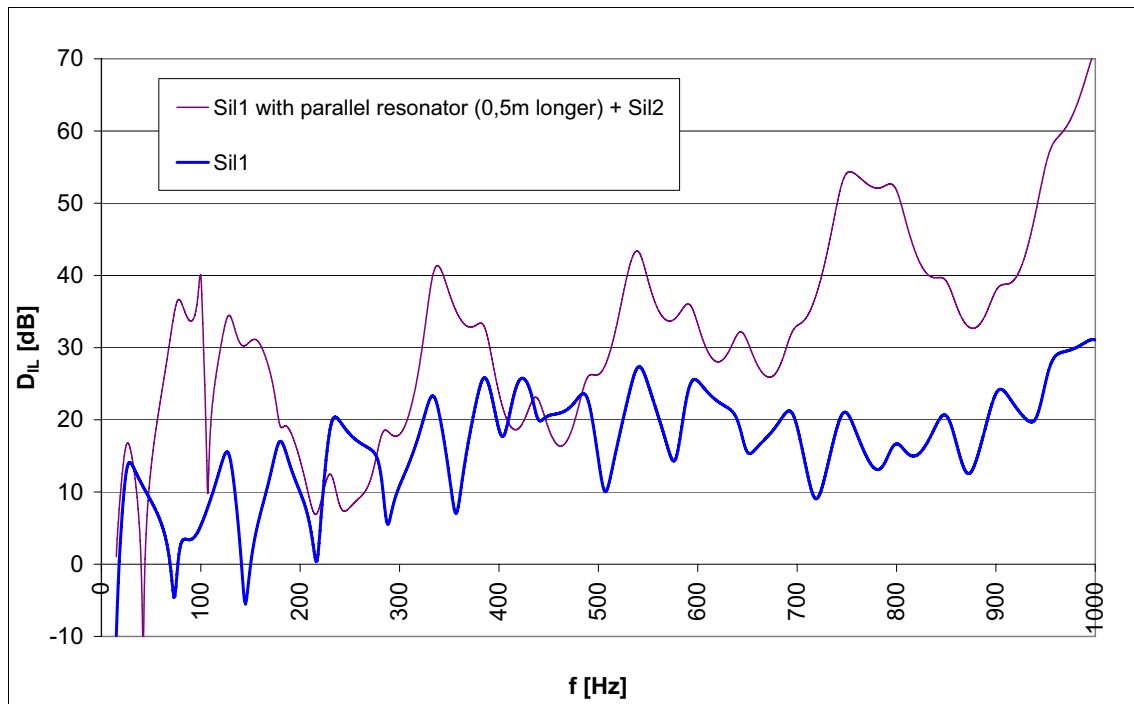


Figure 5.9: Built-in parallel resonator into silencer Sil1 in system sil1+2 compared to system sil1.

showed in figure 5.8. Adding Sil2 to the system then gives that extra attenuation to the frequencies that had increased in D_{IL} due to the use of a parallel resonator. This can be seen in figure 5.9.

5.6.2 Sources of error in the modelling

The following list contains errors that were not possible to correct in this thesis but if actions are taken to rectify these errors the modelling would provide more accurate results.

- When determining the *inlet mass flow* in the unit kg/s the density used was the same as for air. To get a more correct *inlet mass flow* one needs measurements of the diesel engines exhaust and thus get the correct density. This can overestimate or underestimate the peaks at actual frequencies.
- The simulation is difficult at low frequencies where the near field effects in the measurements produce an overestimate of sound pressure levels.
- The source impedance is an estimation based on which numbers gave the best results. A measurement on the complete system with engine and mufflers would provide more scientific weight to the modelling. To achieve this information, the engine and silencers has to be sent to the Marcus Wallenberg Laboratory in Stockholm.
- The existing muffler system has too small dimensions. This makes the system very unstable and thus very sensitive to different source impedances (different engines). This makes the fact that the source impedance is chosen as described above unfortunate. The muffler dimensions should consequently be larger so that the end pipe reflections do not travel through the entire system without being attenuated.

- The claim that the data is insufficient ,made in section (3.3.3), means that there are frequencies where there is good theoretical D_{IL} but nothing in the measured D_{IL} . Reversed, there are places where there are no information in the measurement which makes it very difficult to make a distinction between areas of little D_{IL} or areas of little information.
- Perforated pipes and different insulation materials in the muffler are represented as a flow resistivity are estimated from information in the literature.
- The value of exhaust gas flow is taken from the engines own specifications. Measured values would provide more accuracy to the modelling.
- Some lengths in the system are uncertain, for example the distance between the turbo to the first pipe and how this should be simulated.

6 Summary of results

6.1 Measurement method

The new measuring method, developed in this thesis, provides very useful information. This method is an option which requires only an ordinary microphone and an open field thus allowing the measurement to take place at a company's own premises. Previously, Kalmar Industries AB has only recorded the total sound pressure levels. Doing so, one neglects the individual sound sources and frequency components that are vital for an analysis of the sound.

6.2 Analysis of measuring results

The new measuring method makes it clear that the main silencer is not working well. The method produces highly analysable data for evaluating the efficiency of the truck silencers. Two frequencies are identified to be, by far, most important for the total sound pressure level, 99 Hz and 198 Hz. It is determined that the silencers have very low insertion loss at these peaks, i.e, the silencers are extremely inefficient where they should be efficient. For frequencies higher than 250 Hz the insertion loss is found to be acceptable, however, this is overshadowed by the extreme lack of insertion loss at 99 Hz. Some external sound sources are also identified, making it possible to exclude those frequencies when constructing a new muffler.

6.3 Modelling

The simulation supports the claim that the silencers are inefficient by determining that they are poorly dimensioned. The results from the measurements provide confirmation that the models, made with the simulation tool SIDLAB, of the two existing silencers are correct. By increasing the dimensions of that model it is determined that the main silencer is simply too small.

A simulated implementation of a parallel resonator in the main silencer, tuned to 100 Hz, results in an alternative silencer that greatly improves sound reduction.

All in all, Mathematical modelling based on linearity and one-dimensional interaction between the silencer elements is advantageous and gives very good results when understanding, analysing and simulating the silencer. The conclusion is that SIDLAB works well and saves a lot of time by its fast modelling and easy interface.

A Appendix

A.1 Temperature

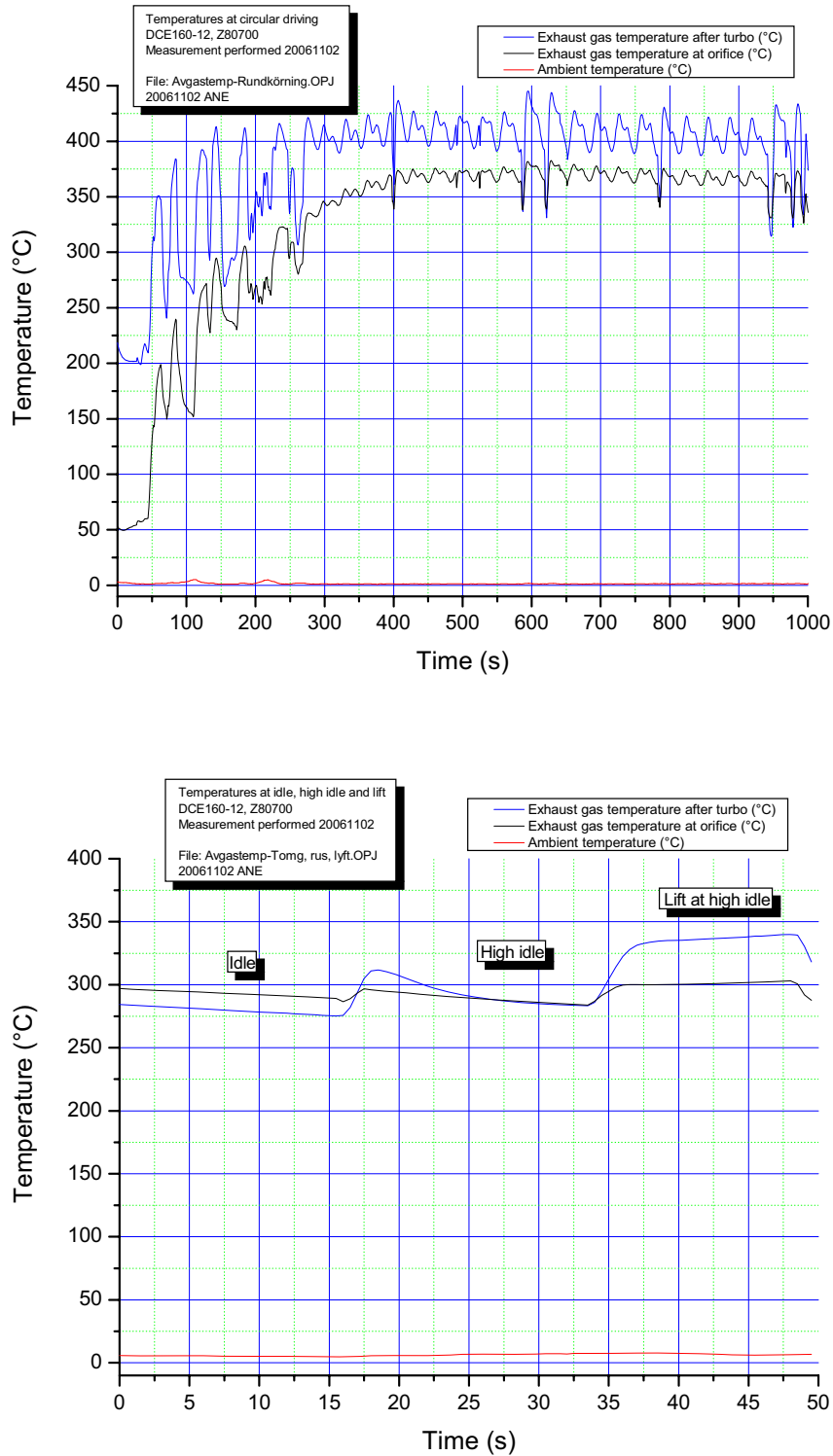


Figure A.1: The top image represents the exhaust gas temperatures at circular driving and the bottom image the exhaust gas temperatures at low idle, high idle and lift.

References

- [1] *Rock wool*. <http://www.bobgolds.com/AbsorptionCoefficients.htm>.
- [2] H Bodén, U Carlsson, R Glav, H P Wallin, and M Åbom. *Ljud och Vibrationer*. Marcus Wallenberg Laboratoriet för Ljud- och Vibrationsforskning, Inst. för Farkostteknik, KTH, 2001.
- [3] M Åbom, R Glav, S Nygård, and T Elnady. *SIDLAB User Manual, Version 1*. Elnady Engineering & Agencies, Cairo, 2006.
- [4] Mats Åbom. *An itroduction to Flow Acoustics*. KTH, Engineering Sciences, 2006.
- [5] Lawrence E. Kinsler et al. *Fundamentals of Acoustics, Fourth edition*. John Wiley SCNS, Inc., 2000.
- [6] B Nilsson and O Brander. *The propagation of sound in cylindrical ducts with mean flow and bulk reacting lining - IV. Several interacting discontinuities*. IMA J. Appl. Math 27, 1981.
- [7] Nygård Stefan. *Modelling of low frequency sound in duct networks*. Marcus Wallenberg Laboratoriet för Ljud- och Vibrationsforskning, KTH, 2000.



Växjö
universitet

Matematiska och systemtekniska institutionen
SE-351 95 Växjö

tel 0470-70 80 00, fax 0470-840 04
www.msi.vxu.se